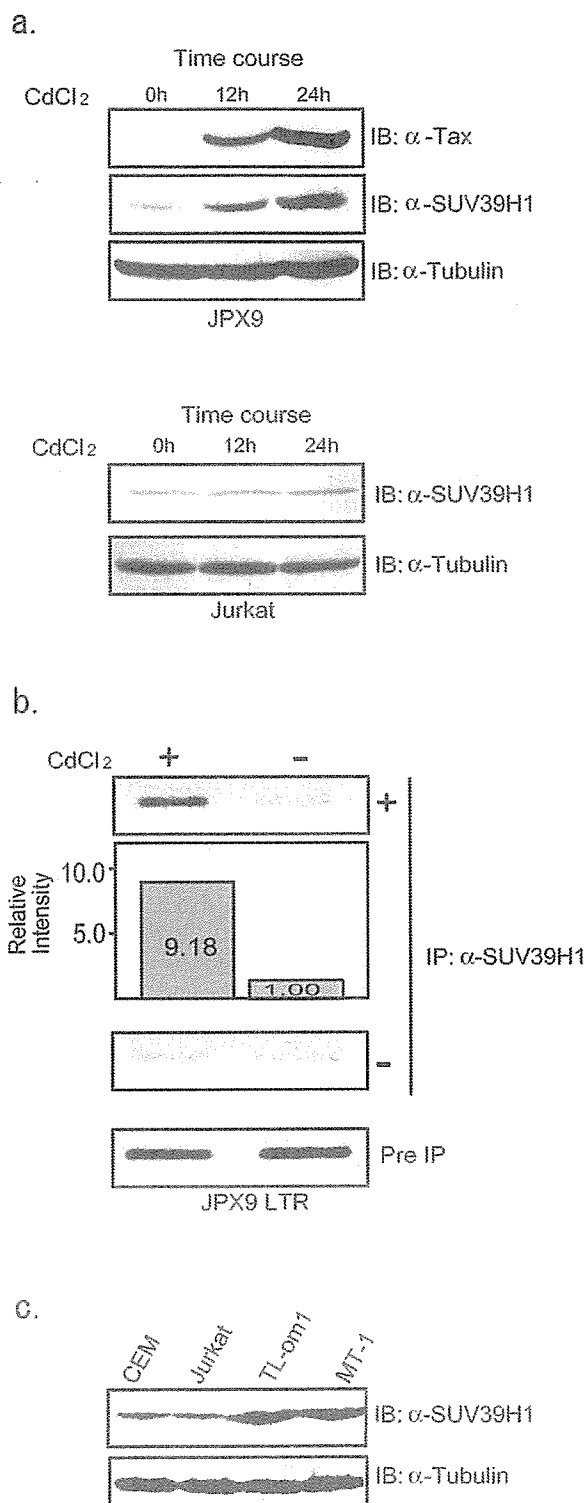
**Figure 5**

SUV39H1 represses Tax transactivation of HTLV-I LTR promoter activity. Representative results of luciferase assays using HEK293 and Jurkat cells (left and right panels, respectively) are shown with the mean and standard deviation of triplicate experiments. Below the graphs, results of immunoblot analyses of whole cell lysates are shown to confirm expression of transduced proteins. (a) Dose-dependent repression of Tax transactivation of HTLV-I LTR by SUV39H1. More than three independent assays were done for each cell line. (b) Effects of SUV39H1 on the basal activities of HTLV-I LTR. In the absence of Tax, increasing amounts of SUV39H1 expression plasmid was transfected with HTLV-I Luc. Left and right panels show the results of HEK293 and Jurkat cells, respectively. (c) Absence of repression of Tax transactivation by HMTase negative SUV39H1. Tax expression plasmid was co-transfected with the wild type or HMTase negative mutant SUV39H1 along with the reporter plasmid pHTLV LTR-Luc. Lower two panels show the results of immunoblot analyses to confirm the expression of transduced Tax and SUV39H1 proteins. Antibodies used are indicated on the left. (d) Suppressing activities of SUV39H1 mutants on Tax transactivation of HTLV-I LTR promoter activity. Fold activation of HTLV LTR promoter activity by Tax is shown with the mean and standard deviation of triplicated experiments. Co-transfected HA-tagged mutant SUV39H1 constructs are indicated below the graph and on the right of lower panels. Structures of these deletion mutants are described in Fig. 2a, upper panel.



**Figure 6**

Induction of SUV39H1 expression in JPX9 cells and localization on the HTLV-I LTR, and endogenous levels of SUV39H1 expression in T cell lines. (a) Top figure: Expression of Tax and SUV39H1 in CdCl<sub>2</sub>-treated JPX9 cells. Whole cell lysates of JPX9 cells treated by CdCl<sub>2</sub> for indicated periods were studied by immunoblot analysis with anti-Tax and anti-SUV39H1 monoclonal antibodies (top and middle panels). The bottom panel shows the immunoblot by anti-tubulin antibody. Bottom figure: Absence of SUV39H1 induction in Jurkat cells by CdCl<sub>2</sub> treatment. Whole cell lysates of Jurkat cells treated by CdCl<sub>2</sub> for indicated periods were studied by immunoblot analysis with anti-SUV39H1 monoclonal antibody (top panel). The bottom panel shows the immunoblot by anti-tubulin antibody. (b) Results of ChIP assays. Representative photographs of agarose gel electrophoresis of PCR products are shown. Top panel shows results of CdCl<sub>2</sub>-treated and untreated JPX9LTR clones. The relative intensities of the band measured by NIH Image software are shown in the second panel. The third and bottom panels show the results of negative controls without first antibody and input controls, respectively. (c) SUV39H1 expression in various T cell lines. ATL-derived cell lines (MT-1 and TL-om1) show higher levels of SUV39H1 expression compared with HTLV-I-uninfected cell lines (top panel). TL-om1 and MT-1 are ATL-derived and HTLV-I-infected cell lines. The bottom panel shows the immunoblot by anti-tubulin antibody.

tional change of the chromatin through H3 K9 methylation can explain the dose-dependent repression of Tax transactivation of LTR by SUV39H1. Taken together with the induction of endogenous SUV39H1 expression by Tax and the recruitment to the LTR, Tax-SUV39H1 interaction may form a negative feedback loop that self-limits HTLV-1 viral gene expression in infected cells

## Materials and methods

### Cell cultures and transfection

Jurkat, HEK293 and HEK293T cell lines were obtained from Fujisaki Cell Biology Center (Okayama, Japan) and the Japanese Cancer Research Resources Bank (Tokyo, Japan). JPX9, a cell line that can be induced to express Tax by CdCl<sub>2</sub> treatment, was a gift from Prof. Sugamura, Tohoku University. Jurkat and HEK293T cells were cultured in RPMI 1640 supplemented with 10% FCS and antibiotics, and in DMEM supplemented with 10% FCS and antibiotics, respectively. For the co-immunoprecipitation and *in vitro* methyltransferase assays, transfection was done by the standard calcium phosphate precipitation method using  $8 \times 10^5$  HEK293T cells and a total of 30  $\mu$ g of expression vectors. An empty expression vector pME18S or pMEG was used for control transfections or to make the total amount of transfected plasmid to be 30  $\mu$ g.

**Plasmids and cDNA**

Human cDNA for SUV39H1 was amplified by RT-PCR from a normal human PBMC cDNA, and used after confirmation of the nucleotide sequence. The primers used for amplification were as follows: SUV39H1-F1: 5'-CCGCTCGAGATGGCGGAAAATTTAAAAGGCTGCAGCGTG-3', SUV39H1-R1: 5'-GGACTAGTCTAGAA-GAGGTATTTGCGGCAGGACTCAGT-3'. GST-fusion proteins of mutants of SUV39H1 that lack functional domains were also prepared using PCR of the wild type cDNA. Forward primers: 5'-AAACTCGAGATGTTCCACAAGGACTTAGAAAAGGGAGCTG-3' ( $\Delta$ N89), 5'-AAACTCGAGATGGTGTACATCAATGAGTACCGTGTGGT-3' (cysSET), Reverse primers, 5'-GGACTAGTGT-CATTGTAGGCCAAACTTGTGCAAGTGACGC-3' (wild type,  $\Delta$ N89, cysSET), 5'-CCCACTAGTTCACCGAAGATGCAGAGGTCATATAGGAT-3' ( $\Delta$ SET), 5'-CCCACTAGTTCACAGGTAGTTGGCCAAGCTTGGGTCCAG-3' (Nchromo), 5'-CCCACTAGTTCACAGGTAGTTGGCCAAGCTTGGGTCCAG-3' (N44). pGEX5X-3 (Amersham) was used to prepare bacterially expressed GST-fusion proteins. For the expression in mammalian cell lines, the following expression vectors were constructed. pMEG, a vector containing the humanized GST protein [50,51], was used to construct pMEG-SUV39H1, which was used for binding assays. pME-Flag-SUV39H1 was used for transient co-transfection and co-immunoprecipitation assays. For functional and immunohistochemical analyses, an expression vector pcDNA-HA-SUV39H1 was used. To prepare an expression vector for a kinase-negative SUV39H1, we mutated histidine codon 324 into a leucine codon according to Lachner et al [40] using PCR with a mutated primer. The region from nucleotide position 961 from ATG to 1239 (end of the stop codon) was amplified using a mutating forward primer (5'-TTTGTCAACCTCAGTTGTGACCCCAACCTGCA-3') and a reverse primer SUV39H1-R1. The amplified fragment replaced the region of the wild type cDNA in pcDNA-HA-SUV39H1 using the *HincII* restriction enzyme site. The resultant plasmid has a mutated cDNA encoding leucine at 324 instead of histidine (H324L) and was named pcDNA-HA-SUV39H1-H324L. GST-fusion proteins were purified using Glutathione Sepharose 4B (Amersham), followed by confirmation with SDS-PAGE and CBB staining. For expression of histidine-tagged Tax protein, pET3d/Tax was prepared, and the fusion protein was purified by ProBond Resin (Invitrogen), followed by confirmation by SDS-PAGE and CBB staining.

**in vitro transcription and translation**

For *in vitro* translation of the wild type and mutant Tax proteins, the cDNA was amplified by PCR and cloned into pBluescript II SK (-). *in vitro* transcription and translation of the indicated cDNA was done using TNT QuickCoupled Transcription/Translation Systems (Promega). The

proteins were labeled by incorporating  $^{35}$ S-Methionine (Amersham), and confirmed by autoradiography of the SDS-PAGE of the products. The primers used are as follows: forward primer for wild type, N180 and  $\Delta$ CBP-B, 5'-TGAATTCCATATGGCCCACTTCCCAGGGTTTGGGA-3', forward primer for  $\Delta$ N108, 5'-TGAATTCCATATGCCCAAATACTCCCCCTTCCGA-3'; reverse primer for wild type, N180 and  $\Delta$ CBP-B, 5'-AAACTCGAGGGATCCGACTTCTGTTTCGCGGAAATGTTT-3', reverse primer for N180, 5'-CCCGAGCTGGCCGGGGTCCGAAAA-3'. A Tax mutant that lacks the CBP binding domain (amino acids 81 to 108) was prepared as follows. First, *SpeI* recognition site was introduced into the nucleotide positions of 238 to 243 and 334 to 339 by Kunkel's method, then the plasmid was digested by *SpeI* and the larger fragment was separated and recovered from agarose gel, followed by self-ligation. The oligonucleotides used for introduction of point mutations are as follows: MS-1: 5'-CTCCCCTCCTTCCCCTAGTAGAACCTCTAAGACC-3', MS-2 5'-CAGGCCATGCGCAAACTAGTCCCTTCCGAAATGGA-3'.

**GST pull-down assay**

Wild type and mutant GST-SUV39H1 proteins (2  $\mu$ g) bound to Glutathione-Sepharose 4B were mixed with His-tagged Tax protein (2  $\mu$ g) in cold PBS and incubated at 4°C for one hour. After centrifugation, proteins bound to Glutathione-Sepharose 4B were separated by 10% SDS-PAGE followed by immunoblot analysis using anti-Tax monoclonal antibody Lt-4. Relative intensities of the bands were determined using the NIH Image software. Binding analyses using *in vitro* translated and  $^{35}$ S-labeled Tax proteins were done basically as described above. The amounts of *in vitro* translation products were one fourth of the reaction mixture. Binding was detected by autoradiography of the dried gel that had been fixed for 30 min in 10% acetic acid, 10% methanol, 10% glycerol followed by treatment with Amplify Fluorographic Reagent (Amersham) for 30 min. Relative intensities of signals were determined by Autoimage Analyzer (BAS2000, Fuji Photo Film, Tokyo).

**Co-immunoprecipitation and immunoblotting**

Immunoblots were done to detect co-immunoprecipitated or GST pull-down proteins, as described previously [52]. For co-immunoprecipitation analyses, cell lysates were prepared in TNE buffer (10 mM Tris-HCl, pH7.8, 1% Nonidet P-40, 150 mM NaCl, 1 mM EDTA). When indicated, aliquots were removed for immunoblots of whole cell lysates. Primary antibodies used were anti-SUV39H1 monoclonal antibody (abcam) and anti-Tax monoclonal antibody Lt-4 [33] and alkaline phosphatase-conjugated anti-mouse immunoglobulin sheep and anti-rabbit donkey antibodies (both from Promega) were used as secondary antibodies.

### Immunohistochemistry

HEK293T cells ( $8 \times 10^5$ ) were grown on coverslips for one day, and transfected with 10  $\mu$ g of pCG-Tax and 20  $\mu$ g of pcDNA-HA-SUV39H1 by the calcium phosphate precipitation method. Jurkat cells ( $2 \times 10^5$ ) were transfected with 2  $\mu$ g each of pCG-Tax and pcDNA-HA-SUV39H1 plasmids using Lipofectamine2000 (Invitrogen). After 36 hours, HEK293T cells were fixed with 4% paraformaldehyde for 10 min at room temperature, followed by permeabilization with 0.1% TritonX. Jurkat cells were harvested and fixed with acetone/methanol (1:1). Both cells were incubated with anti-Tax antibody Lt-4 and/or anti-HA antibody for one hour, followed by washing with PBS and incubation with fluorescence labeled secondary antibodies for one hour. The secondary antibodies used were Alexa Fluor 546 (anti-mouse antibody, Invitrogen) and Alexa Fluor 488 (anti-rabbit antibody, Invitrogen). Cells were fixed on a slide glass using mounting medium (PBS: glycerol, v:v = 1:9) and covered with a FluoroGuard anti-fade reagent (Bio-Rad). Fluorescence signals were detected using confocal microscopy (Radiance 2000, Bio-Rad).

### in vitro HMT assay

The assay was done basically according to the method reported by Fuks et al. [39] with slight modifications. Briefly, SUV39H1 expression vector pME-Flag-SUV39H1 was transfected alone or with Tax expression vector pCG-Tax into HEK293T cells. After culturing for 40 hours, cells were lysed in TNE buffer, followed by immunoprecipitation with anti-FLAG M2 antibody. The immunoprecipitates were used for *in vitro* methyltransferase assay using histone octamer (Sigma) as substrates. Reaction was done at 30°C for indicated time in a reaction buffer containing 50 mM Tris-HCl, pH8.5, 20 mM KCl, 10 mM MgCl<sub>2</sub>, 10 mM  $\beta$ -mercaptoethanol, and 250 mM sucrose in the presence of 10  $\mu$ Ci <sup>3</sup>H-adenosylmethionine (Amersham). The reaction mixture was analyzed by 15% SDS-PAGE. After fixation, gels were treated with Amplify Fluorographic Reagent (Amersham) for 30 min and followed by fluorography. The levels of methylation were evaluated by densitometric analyses of the bands using NIH Image software.

### Reporter Gene Assays

To study the transactivation of HTLV-1 LTR promoter by Tax, reporter gene assays were done, using pHTLV-LTR-Luc plasmid as a reporter and pCG-Tax as an effector in the presence or absence of SUV39H1. pHTLV-LTR-Luc and pCG-Tax were generous gifts from Prof. J Fujisawa, Kansai Medical University [53]. Briefly, a reporter plasmid, pHTLV-LTR-Luc, was constructed by inserting a 647-bp HTLV-1 LTR fragment into the MCS site of the pGL3 vector (Promega). HEK293 cells were transfected with 50 ng of pHTLV-LTR-Luc, 50 ng of pCG-Tax and 10 to 1,000 ng of pcDNA-HA-SUV39H1 by the calcium phosphate

precipitation method. Jurkat cells were transfected with 100 ng of pHTLV-LTR-Luc, 10 ng of pCG-Tax and 10 to 500 ng of pcDNA-HA-SUV39H1 by the DEAE method [50]. A  $\beta$ -galactosidase expression plasmid driven by the  $\beta$ -actin promoter (p $\beta$ -act- $\beta$ -gal) [54] was co-transfected to standardize each experiment. Cells were harvested 48 h after transfection, and Luciferase activity was measured with Luciferase assay kit (Promega). The measured activities were standardized by the activities of  $\beta$ -galactosidase, and transactivation was expressed as fold activation compared with the basal activity of LTR-Luc without effectors such as SUV39H1 or Tax. Representative results of triplicate experiments that were repeated more than three times are shown in the figures with the mean and standard deviation.

### Induction of Tax expression in JPX9 cells

JPX9 cells were cultured in RPMI1640 supplemented with 10% FCS and antibiotics unless stimulated with CdCl<sub>2</sub>. Tax expression in JPX9 cells was induced by culturing  $1 \times 10^6$  cells in the presence of 30  $\mu$ M CdCl<sub>2</sub> for indicated hours. Then, cells were harvested and lysed by  $1 \times$  sample buffer (65 mM Tris-HCl pH 6.8, 3% SDS, 10% glycerol, 0.01% BPB) followed by 10 min of boiling. Samples corresponding to  $2 \times 10^5$  cells were separated by SDS-PAGE and transferred to PVDF membrane as described above. After blocking with skim milk, the membranes were incubated with the primary antibody at room temperature for one hour, washed in TBST buffer and incubated with the alkaline phosphatase-conjugated anti-mouse secondary antibody at room temperature for one hour. The primary antibodies used are as follows: anti-SUV39H1 mouse monoclonal antibody (abcam), anti-Tax mouse monoclonal antibody Lt-4, and anti-tubulin mouse monoclonal antibody (Santa Cruz).

### Chromatin immunoprecipitation (ChIP) assays

To examine the tethering of SUV39H1 by Tax, we prepared JPX9 transformants that were stably transfected with the HTLV-1 LTR Luc plasmid and pA-puro plasmid. After cloning by limiting dilution, isolated clones were tested for induction of Tax expression and luciferase activities by CdCl<sub>2</sub> treatment, and selected clones were named JPX9LTR clones (Detailed analyses using these clones will be reported in a separate paper). Using three JPX9 LTR clones, ChIP assays were performed to test tethering of SUV39H1 to the HTLV-1 LTR after Tax expression. Cells ( $2 \times 10^6$  per clone) were treated with or without CdCl<sub>2</sub> for 48 hours followed by cross-linking at 37°C for 10 min with formaldehyde (1% final concentration). Cells were pelleted by centrifugation and resuspended in 1 ml of ice-cold PBS (-) with protease inhibitor cocktail (Sigma). Cells were again pelleted by centrifugation at 4°C. The pellet was suspended in 500  $\mu$ l of the lysis buffer (1% SDS, 10 mM EDTA, 50 mM Tris-HCl [pH8.1]) and kept on

ice for 10 min. After sonication on ice with an Astrason Ultrasonic Processor (Misonix) to shear DNA to lengths of between 200 and 1,000 bp (as estimated by agarose gel electrophoresis), lysates were cleared by centrifugation. The supernatant was then diluted 10-fold with dilution buffer (0.01% SDS, 1.1% Triton, 1.2 mM EDTA, 16.7 mM Tris-HCl [pH 8.1], 16.7 mM NaCl) with protease inhibitors to a final volume of 5 ml. An aliquot (500 µl) of the supernatant was saved to represent unfractionated chromatin. The diluted cell supernatant was precleared with a 50% suspension of protein G Sepharose beads (Sigma) for 30 minutes at 4°C with agitation. Sepharose was pelleted by brief centrifugation and the supernatant was transferred to a new tube. The cross-linked chromatin suspension was mixed with anti-SUV39H1 antibody or PBS as negative controls, and incubated overnight at 4°C. Immune complexes were reacted for 1 h at 4°C with agitation with a 50% suspension of protein G-Sepharose beads equilibrated with dilution buffer. After the reaction, the beads were collected and washed serially with the following buffers: buffer a [0.1% SDS, 1% Triton X-100, 2 mM EDTA, 20 mM Tris-HCl [pH 8.1], 150 mM NaCl], buffer b [0.1% SDS, 1% Triton X-100, 2 mM EDTA, 20 mM Tris-HCl [pH 8.1], 500 mM NaCl], buffer c [0.25 M LiCl, 1% NP-40, 1% Sodium Deoxycholate, 1 mM EDTA, 10 mM Tris-HCl [pH 8.1], and TE. Immune complexes were eluted twice with 250 µl of elution buffer (1% SDS, 0.1 M NaHCO<sub>3</sub>) for 15 min at room temperature and 20 µl of 5 M NaCl was added to the 500 µl eluates. Cross-links were reversed by heating at 65°C for 4 h, followed by addition of 10 µl 0.5 M EDTA, 20 µl 1 M Tris-HCl [pH 6.5], and incubated at 45°C for 1 h in the presence of 40 µg/ml of proteinase K. The DNA was purified by phenol/chloroform extraction followed by ethanol precipitation. The recovered DNA was resuspended in 50 µl of TE. PCR was performed in 50 µl with Ampli Taq (Perkin-Elmer) and for 35 cycles (annealing temperature is 55°C). The set of primers used was as follows; forward 5'-ACA-GAAGTCTGAGAAGGTCA -3' and reverse 5'-TGGGTGGT-TCCCGGTGGCTT -3'. The predicted PCR product length is 150 bp. All PCR signals stained with Ethidium Bromide on 2.0% agarose gel were quantified with the NIH Image software.

#### Competing interests

The author(s) declare that they have no competing interests.

#### Authors' contributions

KK carried out co-immunoprecipitation assays, confocal immunofluorescence analysis and reporter gene assays, and prepared the figures. KY participated in construction of mutant expression plasmids, and performed *in vitro* binding assays. Aya M participated in construction of a methyltransferase negative mutant of SUV39H1 per-

formed a part of reporter gene assays. Ari M prepared JPK9 LTR clones and performed ChIP assays. TI participated in the experimental design and data analysis, and performed *in vitro* HMTase assays. YT provided anti-Tax monoclonal antibody Lt-4 and contributed to experimental design and data analysis. MM participated in the experimental design, data analysis and writing of the manuscript. TW conceived of the study, and participated in its design and coordination, and data analysis, as well as in writing the manuscript. All authors have read and approved the final manuscript.

#### Acknowledgements

We thank Prof. Jun-ichi Fujisawa for pCG-Tax and pHTLV-LTR-Luc plasmids, and Ms A. Hamano and Ms M. Maruyama-Nagai for helping our work. This work was supported by Grants-in-Aid for Scientific Research from Ministry of Education, Culture, Sports, Science and Technology of Japan to T. Ishida and T. Watanabe.

#### References

- Poiesz BJ, Ruscetti FW, Gazdar AF, Bunn PA, Minna JD, Gallo RC: **Detection and isolation of type C retrovirus particles from fresh and cultured lymphocytes of a patient with cutaneous T-cell lymphoma.** *Proc Natl Acad Sci U S A* 1980, **77**:7415-7419.
- Yoshida M, Miyoshi I, Hinuma Y: **Isolation and characterization of retrovirus from cell lines of human adult T-cell leukemia and its implication in the disease.** *Proc Natl Acad Sci U S A* 1982, **79**:2031-2035.
- Yamaguchi K, Watanabe T: **Human T lymphotropic virus type-I and adult T-cell leukemia in Japan.** *Int J Hematol* 2002, **76 Suppl 2**:240-245.
- Watanabe T: **HTLV-I-associated diseases.** *Int J Hematol* 1997, **66**:257-278.
- Koiwa T, Hamano-Usami A, Ishida T, Okayama A, Yamaguchi K, Kamihira S, Watanabe T: **5'-long terminal repeat-selective CpG methylation of latent human T-cell leukemia virus type I provirus *in vitro* and *in vivo*.** *J Virol* 2002, **76**:9389-9397.
- Hironaka N, Mochida K, Mori N, Maeda M, Yamamoto N, Yamaoka S: **Tax-independent constitutive IκappaB kinase activation in adult T-cell leukemia cells.** *Neoplasia* 2004, **6**:266-278.
- Gatza ML, Watt JC, Marriott SJ: **Cellular transformation by the HTLV-I Tax protein, a jack-of-all-trades.** *Oncogene* 2003, **22**:5141-5149.
- Yoshida M: **Multiple viral strategies of HTLV-I for dysregulation of cell growth control.** *Annu Rev Immunol* 2001, **19**:475-496.
- Mesnard JM, Devaux C: **Multiple control levels of cell proliferation by human T-cell leukemia virus type I Tax protein.** *Virology* 1999, **257**:277-284.
- Bex F, Gaynor RB: **Regulation of gene expression by HTLV-I Tax protein.** *Methods* 1998, **16**:83-94.
- Suzuki T, Fujisawa JI, Toita M, Yoshida M: **The trans-activator tax of human T-cell leukemia virus type I (HTLV-I) interacts with cAMP-responsive element (CRE) binding and CRE modulator proteins that bind to the 21-base-pair enhancer of HTLV-I.** *Proc Natl Acad Sci U S A* 1993, **90**:610-614.
- Zhao LJ, Giam CZ: **Human T-cell lymphotropic virus type I (HTLV-I) transcriptional activator, Tax, enhances CREB binding to HTLV-I 21-base-pair repeats by protein-protein interaction.** *Proc Natl Acad Sci U S A* 1992, **89**:7070-7074.
- Bantignies F, Rousset R, Desbois C, Jalinet P: **Genetic characterization of transactivation of the human T-cell leukemia virus type I promoter: Binding of Tax to Tax-responsive element I is mediated by the cyclic AMP-responsive members of the CREB/ATF family of transcription factors.** *Mol Cell Biol* 1996, **16**:2174-2182.
- Shnyreva M, Munder T: **The oncoprotein Tax of the human T-cell leukemia virus type I activates transcription via interaction with cellular ATF-1/CREB factors in *Saccharomyces cerevisiae*.** *J Virol* 1996, **70**:7478-7484.

15. Kwok RP, Laurance ME, Lundblad JR, Goldman PS, Shih H, Connor LM, Marriott SJ, Goodman RH: **Control of cAMP-regulated enhancers by the viral transactivator Tax through CREB and the co-activator CBP.** *Nature* 1996, **380**:642-646.
16. Riou P, Bex F, Gazzolo L: **The human T cell leukemia/lymphotropic virus type I Tax protein represses MyoD-dependent transcription by inhibiting MyoD-binding to the KIX domain of p300. A potential mechanism for Tax-mediated repression of the transcriptional activity of basic helix-loop-helix factors.** *J Biol Chem* 2000, **275**:10551-10560.
17. Vo N, Goodman RH: **CREB-binding protein and p300 in transcriptional regulation.** *J Biol Chem* 2001, **276**:13505-13508.
18. Fry CJ, Peterson CL: **Transcription. Unlocking the gates to gene expression.** *Science* 2002, **295**:1847-1848.
19. Pise-Masison CA, Mahieux R, Radonovich M, Jiang H, Brady JN: **Human T-lymphotropic virus type I Tax protein utilizes distinct pathways for p53 inhibition that are cell type-dependent.** *J Biol Chem* 2001, **276**:200-205.
20. Ego T, Ariumi Y, Shimotohno K: **The interaction of HTLV-I Tax with HDAC1 negatively regulates the viral gene expression.** *Oncogene* 2002, **21**:7241-7246.
21. Goll MG, Bestor TH: **Histone modification and replacement in chromatin activation.** *Genes Dev* 2002, **16**:1739-1742.
22. Zhang Y, Reinberg D: **Transcription regulation by histone methylation: interplay between different covalent modifications of the core histone tails.** *Genes Dev* 2001, **15**:2343-2360.
23. Jenuwein T, Allis CD: **Translating the histone code.** *Science* 2001, **293**:1074-1080.
24. Strahl BD, Allis CD: **The language of covalent histone modifications.** *Nature* 2000, **403**:41-45.
25. Turner BM: **Cellular memory and the histone code.** *Cell* 2002, **111**:285-291.
26. Litt MD, Simpson M, Gaszner M, Allis CD, Felsenfeld G: **Correlation between histone lysine methylation and developmental changes at the chicken beta-globin locus.** *Science* 2001, **293**:2453-2455.
27. Noma K, Allis CD, Grewal SI: **Transitions in distinct histone H3 methylation patterns at the heterochromatin domain boundaries.** *Science* 2001, **293**:1150-1155.
28. Tachibana M, Sugimoto K, Fukushima T, Shinkai Y: **Set domain-containing protein, G9a, is a novel lysine-preferring mammalian histone methyltransferase with hyperactivity and specific selectivity to lysines 9 and 27 of histone H3.** *J Biol Chem* 2001, **276**:25309-25317.
29. Aagaard L, Laible G, Selenko P, Schmid M, Dorn R, Schotta G, Kuhfitz S, Wolf A, Lebersorger A, Singh PB, Reuter G, Jenuwein T: **Functional mammalian homologues of the Drosophila PEV-modifier Su(var)3-9 encode centromere-associated proteins which complex with the heterochromatin component M31.** *Embo J* 1999, **18**:1923-1938.
30. Huang N, vom Baur E, Garnier JM, Lerouge T, Vonesch JL, Lutz Y, Chambon P, Losson R: **Two distinct nuclear receptor interaction domains in NSD1, a novel SET protein that exhibits characteristics of both corepressors and coactivators.** *Embo J* 1998, **17**:3398-3412.
31. Melcher M, Schmid M, Aagaard L, Selenko P, Laible G, Jenuwein T: **Structure-function analysis of SUV39H1 reveals a dominant role in heterochromatin organization, chromosome segregation, and mitotic progression.** *Mol Cell Biol* 2000, **20**:3728-3741.
32. Sewalt RG, Lachner M, Vargas M, Hamer KM, den Blaauwen JL, Hendrix T, Melcher M, Schweizer D, Jenuwein T, Otte AP: **Selective interactions between vertebrate polycomb homologs and the SUV39H1 histone lysine methyltransferase suggest that histone H3-K9 methylation contributes to chromosomal targeting of Polycomb group proteins.** *Mol Cell Biol* 2002, **22**:5539-5553.
33. Tanaka Y, Yoshida A, Takayama Y, Tsujimoto H, Tsujimoto A, Hayami M, Tozawa H: **Heterogeneity of antigen molecules recognized by anti-tax1 monoclonal antibody Lt-4 in cell lines bearing human T cell leukemia virus type I and related retroviruses.** *Jpn J Cancer Res* 1990, **81**:225-231.
34. Rea S, Eisenhaber F, O'Carroll D, Strahl BD, Sun ZW, Schmid M, Opravil S, Mechtler K, Ponting CP, Allis CD, Jenuwein T: **Regulation of chromatin structure by site-specific histone H3 methyltransferases.** *Nature* 2000, **406**:593-599.
35. Chakraborty S, Sinha KK, Senyuk V, Nucifora G: **SUV39H1 interacts with AML1 and abrogates AML1 transactivity. AML1 is methylated in vivo.** *Oncogene* 2003, **22**:5229-5237.
36. Bex F, McDowall A, Burny A, Gaynor R: **The human T-cell leukemia virus type I transactivator protein Tax colocalizes in unique nuclear structures with NF-kappaB proteins.** *J Virol* 1997, **71**:3484-3497.
37. Semmes OJ, Jeang KT: **Localization of human T-cell leukemia virus type I tax to subnuclear compartments that overlap with interchromatin speckles.** *J Virol* 1996, **70**:6347-6357.
38. Smith MR, Greene WC: **Characterization of a novel nuclear localization signal in the HTLV-I tax transactivator protein.** *Virology* 1992, **187**:316-320.
39. Fuks F, Hurd PJ, Deplus R, Kouzarides T: **The DNA methyltransferases associate with HPI and the SUV39H1 histone methyltransferase.** *Nucleic Acids Res* 2003, **31**:2305-2312.
40. Lachner M, O'Carroll D, Rea S, Mechtler K, Jenuwein T: **Methylation of histone H3 lysine 9 creates a binding site for HPI proteins.** *Nature* 2001, **410**:116-120.
41. Nagata K, Ohtani K, Nakamura M, Sugamura K: **Activation of endogenous c-fos proto-oncogene expression by human T-cell leukemia virus type I-encoded p40tax protein in the human T-cell line, Jurkat.** *J Virol* 1989, **63**:3220-3226.
42. Harrod R, Tang Y, Nicot C, Lu HS, Vassilev A, Nakatani Y, Giam CZ: **An exposed KID-like domain in human T-cell lymphotropic virus type I Tax is responsible for the recruitment of coactivators CBP/p300.** *Mol Cell Biol* 1998, **18**:5052-5061.
43. Chun AC, Zhou Y, Wong CM, Kung HF, Jeang KT, Jin DY: **Coiled-coil motif as a structural basis for the interaction of HTLV type I Tax with cellular cofactors.** *AIDS Res Hum Retroviruses* 2000, **16**:1689-1694.
44. Tie F, Adya N, Greene WC, Giam CZ: **Interaction of the human T-lymphotropic virus type I Tax dimer with CREB and the viral 21-base-pair repeat.** *J Virol* 1996, **70**:8368-8374.
45. Burton M, Upadhyaya CD, Maier B, Hope TJ, Semmes OJ: **Human T-cell leukemia virus type I Tax shuttles between functionally discrete subcellular targets.** *J Virol* 2000, **74**:2351-2364.
46. Vaute O, Nicolas E, Vandel L, Trouche D: **Functional and physical interaction between the histone methyl transferase Suv39H1 and histone deacetylases.** *Nucleic Acids Res* 2002, **30**:475-481.
47. Fujita N, Watanabe S, Ichimura T, Tsuruzoe S, Shinkai Y, Tachibana M, Chiba T, Nakao M: **Methyl-CpG binding domain I (MBD1) interacts with the Suv39H1-HPI heterochromatic complex for DNA methylation-based transcriptional repression.** *J Biol Chem* 2003, **278**:24132-24138.
48. Vandel L, Nicolas E, Vaute O, Ferreira R, Ait-Si-Ali S, Trouche D: **Transcriptional repression by the retinoblastoma protein through the recruitment of a histone methyltransferase.** *Mol Cell Biol* 2001, **21**:6484-6494.
49. Aagaard L, Schmid M, Warburton P, Jenuwein T: **Mitotic phosphorylation of SUV39H1, a novel component of active centromeres, coincides with transient accumulation at mammalian centromeres.** *J Cell Sci* 2000, **113** ( Pt 5):817-829.
50. Ishida T, Mizushima S, Azuma S, Kobayashi N, Tojo T, Suzuki K, Aizawa S, Watanabe T, Mosialos G, Kieff E, Yamamoto T, Inoue J: **Identification of TRAF6, a novel tumor necrosis factor receptor-associated factor protein that mediates signaling from an amino-terminal domain of the CD40 cytoplasmic region.** *J Biol Chem* 1996, **271**:28745-28748.
51. Ishida TK, Tojo T, Aoki T, Kobayashi N, Ohishi T, Watanabe T, Yamamoto T, Inoue J: **TRAF5, a novel tumor necrosis factor receptor-associated factor family protein, mediates CD40 signaling.** *Proc Natl Acad Sci U S A* 1996, **93**:9437-9442.
52. Horie R, Ito K, Tatewaki M, Nagai M, Aizawa S, Higashihara M, Ishida T, Inoue J, Takizawa H, Watanabe T: **A variant CD30 protein lacking extracellular and transmembrane domains is induced in HL-60 by tetradecanoylphorbol acetate and is expressed in alveolar macrophages.** *Blood* 1996, **88**:2422-2432.
53. Furuta RA, Sugiura K, Kawakita S, Inada T, Ikehara S, Matsuda T, Fujisawa J: **Mouse model for the equilibration interaction between the host immune system and human T-cell leukemia virus type I gene expression.** *J Virol* 2002, **76**:2703-2713.
54. Ishida T, Yamauchi K, Ishikawa K, Yamamoto T: **Molecular cloning and characterization of the promoter region of the human c-erbA alpha gene.** *Biochem Biophys Res Commun* 1993, **191**:831-839.

## Transactivation of the *ICAM-1* gene by CD30 in Hodgkin's lymphoma

Jun-Nosuke Uchihara<sup>1,2</sup>, Takehiro Matsuda<sup>1,3</sup>, Taeko Okudaira<sup>1,2</sup>, Chie Ishikawa<sup>1,3</sup>, Masato Masuda<sup>2</sup>, Ryouichi Horie<sup>4</sup>, Toshiki Watanabe<sup>5</sup>, Takao Ohta<sup>5</sup>, Nobuyuki Takasu<sup>2</sup> and Naoki Mori<sup>1\*</sup>

<sup>1</sup>Division of Molecular Virology and Oncology, Graduate School of Medicine, University of the Ryukyus, Nishihara, Japan

<sup>2</sup>Division of Endocrinology and Metabolism, Faculty of Medicine, University of the Ryukyus, Nishihara, Japan

<sup>3</sup>Division of Child Health and Welfare, Faculty of Medicine, University of the Ryukyus, Nishihara, Japan

<sup>4</sup>Fourth Department of Internal Medicine, School of Medicine, Kitasato University, Sagami, Japan

<sup>5</sup>Laboratory of Tumor Cell Biology, Graduate School of Frontier Sciences, The University of Tokyo, Tokyo, Japan

The ICAM-1/LFA-1 complex mediates cell–cell interaction. ICAM-1 is overexpressed in Hodgkin/Reed-Sternberg (H/RS) cells, and serum levels of its soluble form are higher in Hodgkin's lymphoma (HL) patients than in controls. There are no data, however, regarding the regulation of expression of ICAM-1 in H/RS cells. CD30 was identified in H/RS cells of HL and has attracted much interest as a molecular marker of HL. To analyze ICAM-1 expression in H/RS cells, we examined the expression of ICAM-1, LFA-1, CD30 and CD30L in HL-derived cell lines. All cell lines expressed ICAM-1 and CD30, but not LFA-1 or CD30L. CD30 induced ICAM-1 expression. Analysis of the ICAM-1 promoter showed the importance of NF- $\kappa$ B binding site for CD30-induced *ICAM-1* gene expression. Coexpression of I $\kappa$ B, IKK, NIK and TRAF dominant-negative constructs with CD30 inhibited CD30-induced activation of ICAM-1 promoter, suggesting that CD30 induces ICAM-1 via NF- $\kappa$ B signalling. The ICAM-1 promoter was activated by the C-terminal region of CD30, which activated NF- $\kappa$ B signalling. A decoy CD30 lacking the cytoplasmic region inhibited ICAM-1 promoter activity in HL cell lines. Thus, in H/RS cells, ligand-independent activation of CD30 signalling activates NF- $\kappa$ B and this leads to constitutive ICAM-1 expression, suggesting a link between 2 well known phenotypic characteristics of HL, CD30 and ICAM-1 overexpression.

© 2005 Wiley-Liss, Inc.

**Key words:** ICAM-1; CD30; NF- $\kappa$ B; Hodgkin's lymphoma; TRAF

Hodgkin's lymphoma (HL) is characterized by the presence of a few malignant Hodgkin/Reed-Sternberg (H/RS) cells surrounded by dense non-neoplastic infiltrating cells. The non-neoplastic infiltrate is made up of many cell types, including lymphocytes, plasma cells, granulocytes and macrophages.<sup>1</sup> H/RS cells and their neighbors interact *via* a complex network of cellular activation, adhesion molecules and cytokines.<sup>2</sup> It has become evident that inflammatory cells provide factors that support tumor development and thus facilitate the stepwise evolution of a malignant clone.<sup>3</sup> Adhesion molecules play a crucial role in the immune system by promoting cell–cell and cell–stroma interactions and leukocyte trafficking.<sup>4</sup> ICAM-1<sup>5</sup> is a cell adhesion molecule identified as a ligand of LFA-1,<sup>6</sup> and is overexpressed by H/RS cells.<sup>7</sup> Serum levels of soluble ICAM-1 are elevated in HL,<sup>8</sup> and correlate with stage, disease activity and survival.<sup>9,10</sup>

It is of particular interest that several members of the TNF receptor superfamily are highly expressed by H/RS cells, whereas their corresponding cognates are mainly expressed on activated T cells frequently associated with H/RS cells, *e.g.*, CD27/CD27L, CD30/CD30L, CD40/CD40L and CD95/CD95L, indicating a critical role for these molecules in maintaining the local tumor milieu.<sup>11</sup> For example, CD30 is detected consistently on H/RS cells.<sup>12</sup> CD30 was reported initially as “a molecule specific for H/RS cells” that was recognized by monoclonal antibody Ki-1 on the cell surface of H/RS cells. Ki-1 was generated by immunization of mice with the HL cell line L428.<sup>13</sup> Increased serum levels of soluble CD30 correlate with disease activity and thus bear prognostic significance in HL.<sup>14</sup> A later study, however, showed that CD30 was expressed not only on H/RS cells but also on a subset of large cell non-Hodgkin's lymphomas, activated lymphocytes and virus-infected lymphocytes.<sup>15</sup> In contrast, expression of its

ligand CD30L is broader, being expressed on lymphocytes, neutrophils and eosinophils as well as activated monocytes/macrophages.<sup>16,17</sup>

The functional role of CD30 under physiological conditions is not fully understood. At a clonal level, CD30 signals are pleiotropic. In lymphoma cell lines, binding of CD30L to CD30 can induce apoptosis<sup>18,19</sup> or enhance cell proliferation.<sup>18,20</sup> CD30 mediates NF- $\kappa$ B activation<sup>21</sup> and induces cytokine production in the presence or absence of T cell receptor signals.<sup>22</sup> Ligand of TNF superfamily members with their receptors, such as CD30, CD40 and TNF receptor, induces recruitment of TRAF proteins to the cytoplasmic tail of the receptor, and transduces signals to activate IKK that phosphorylates I $\kappa$ B $\alpha$ , the result being translocation of active NF- $\kappa$ B into the nucleus.<sup>23</sup> Ligand-ligated CD30 recruits downstream signal-transducing molecule TRAF proteins, TRAF2 and TRAF5.<sup>24–27</sup> Overexpression of CD30 has been recently reported to transduce signals independent of CD30L.<sup>28</sup>

In our study, we investigated the link between 2 major characteristics of H/RS cells, that is, CD30 overexpression and constitutive ICAM-1 expression. We show that constitutive CD30 signalling partly mediates constitutive ICAM-1 expression in HL.

### Material and methods

#### Cell culture

HL cell lines, L428, KM-H2, HDLM-2 and L540, were cultured in RPMI 1640 medium supplemented with 10% FBS (JRH Biosciences, Lenexa, KS) and antibiotics. Human embryonic kidney 293T cells were maintained in DMEM supplemented with 10% FBS and antibiotics. Peripheral blood mononuclear cells from healthy volunteers were isolated by Ficoll-Paque gradient centrifugation (Amersham Biosciences, Uppsala, Sweden). Mononuclear cells were stimulated with PHA (10  $\mu$ g/ml) for 72 hr.

#### Plasmids and transfections

The expression plasmids human CD30 and its mutant (CD30 $\Delta$ 95) were as described elsewhere.<sup>27</sup> I $\kappa$ B $\alpha$  $\Delta$ N<sup>29</sup> and I $\kappa$ B $\beta$  $\Delta$ N<sup>30</sup> (kindly provided by Dr. D.W. Ballard, Vanderbilt Uni-

**Abbreviations:** EMSA, electrophoretic mobility shift assay; FITC, fluorescein isothiocyanate; HL, Hodgkin's lymphoma; H/RS, Hodgkin/Reed-Sternberg; ICAM-1, intercellular adhesion molecule-1; IKK, I $\kappa$ B kinase; IL-2R, interleukin-2 receptor; LFA-1, leucocyte function-associated antigen-1; NIK, NF- $\kappa$ B-inducing kinase; PBL, peripheral blood lymphocytes; PE, phycoerythrin; PHA, phytohemagglutinin; RT-PCR, reverse transcription-PCR; TK, thymidine kinase; TNF, tumor necrosis factor; TRAF, tumor necrosis factor receptor-associated factor.

Grant sponsor: Ministry of Education, Culture, Sports, Science and Technology; Grant number: 16017289; Grant sponsor: Japan Society for the Promotion of Science; Grant number: 16590951.

\*Correspondence to: Naoki Mori, Division of Molecular Virology and Oncology, Graduate School of Medicine, University of the Ryukyus, 207 Uehara, Nishihara, Okinawa 903-0215, Japan. Fax: +81-98-895-1410. E-mail: n-mori@med.u-ryukyu.ac.jp

Received 12 January 2005; Accepted after revision 16 June 2005

DOI 10.1002/ijc.21427

Published online 8 September 2005 in Wiley InterScience (www.interscience.wiley.com).

versity School of Medicine, Nashville, TN) are deletion mutants of I $\kappa$ B $\alpha$  and I $\kappa$ B $\beta$  lacking the N-terminal 36 amino acids and 23 amino acids, respectively. The kinase-deficient K44M IKK $\alpha$ , K44A IKK $\beta$  and KK429/430AA NIK mutants (kindly provided by Dr. R. Gelezianus, Merck and Company Inc., West Point, PA) have been described previously.<sup>31</sup> Plasmids for truncated TRAF2 and TRAF5 proteins retaining only the TRAF domain were as described previously.<sup>26</sup> The various ICAM-1 promoter constructs (kindly provided by Dr. C. Stratowa, Boehringer Ingelheim Austria, Vienna, Austria and Dr. T.P. Parks, Boehringer Ingelheim Pharmaceuticals Inc., Ridgefield, CT) described previously<sup>32,33</sup> were used to map CD30-responsive regions. Approximately  $5 \times 10^6$  L428, KM-H2 and HDLM-2 cells were electroporated at 960  $\mu$ F and 250 V. 293T cells, at  $3 \times 10^5$  cells per plate, were transfected by the calcium phosphate DNA coprecipitation method. All transfections included appropriate reporter and effector plasmids. To normalize transfection efficiencies, a TK promoter-driven *Renilla* luciferase plasmid (phRL-TK; Promega, Madison, WI) was cotransfected as an internal control plasmid. After 24 hr, transfected cells were collected by centrifugation, washed with PBS and lysed in reporter lysis buffer (Promega). Lysates were assayed for reporter gene activity with the dual luciferase reporter assay system (Promega). Luciferase activities were normalized based on the *Renilla* luciferase activity from phRL-TK.

#### RT-PCR

Total cellular RNA was extracted with Trizol (Invitrogen Corp., Carlsbad, CA) according to the protocol provided by the manufacturer. First-strand cDNA was synthesized from 1  $\mu$ g total cellular RNA using an RNA PCR kit (Takara Shuzo, Kyoto, Japan) with random primers. Thereafter, cDNA was amplified for 35 cycles for CD30, CD30L and ICAM-1 and 28 cycles for  $\beta$ -actin. The oligonucleotide primers used were as follows: for CD30, sense, 5'-CTGTGTCCCCTACCCAATCT-3' and antisense, 5'-CTTCTTTCCTTCTCTTCCA-3';<sup>34</sup> for CD30L, sense, 5'-CCCTCC-TGGAGACACAGC-3' and antisense, 5'-CCTGAAGGCCAAGAGAAACTG-3';<sup>34</sup> for ICAM-1, sense, 5'-TGACCATCTACAGCTTTCGGC-3' and antisense, 5'-AGCCTGGCACATTGGAGTCTG-3';<sup>35</sup> and for  $\beta$ -actin, sense, 5'-GTGGGGCGCCCCAGG-CACCA-3' and antisense, 5'-CTCCTTAATGTCACGCACGAT-TTC-3'. Product sizes were 860 bp for CD30, 690 bp for CD30L, 350 bp for ICAM-1 and 548 bp for  $\beta$ -actin. Cycling conditions were as follows: denaturing at 94°C for 45 sec (for CD30 and CD30L), for 60 sec (for ICAM-1) or for 30 sec (for  $\beta$ -actin), annealing at 62°C for 45 sec (for CD30 and CD30L), 65°C for 120 sec (for ICAM-1), or 60°C for 30 sec (for  $\beta$ -actin) and extension at 72°C for 60 sec (for CD30, CD30L and ICAM-1) or for 90 sec (for  $\beta$ -actin). The PCR products were fractionated on 2% agarose gels and visualized by ethidium bromide staining.

#### Flow cytometry

Cells were washed with cell WASH (Becton Dickinson Immunocytometry Systems, San Jose, CA) and incubated for 30 min with PE-labeled mouse monoclonal antibody against CD30 (clone HRS4) and FITC-labeled mouse monoclonal antibody against ICAM-1 (CD54) (clone 84H10) and LFA-1  $\alpha$  chain (CD11a) (clone 25.3) or control mouse IgG1. These monoclonal antibodies and control mouse IgG1 were purchased from Coulter Immunotech Co. (Marseille, France). Cells were analyzed on a FACS Caliber (Becton Dickinson) after gating on forward and side scatter to exclude debris and clumps, using CellQuest software.

#### Nuclear extracts preparation and EMSA

NF- $\kappa$ B binding activity to NF- $\kappa$ B elements was examined by EMSA, as described previously.<sup>26</sup> In brief, 5  $\mu$ g of nuclear extracts were preincubated in a binding buffer containing 1  $\mu$ g poly-deoxy-inosinic-deoxy-cytidylic acid (Pharmacia, Piscataway, NJ) followed by addition of [ $\alpha$ -<sup>32</sup>P]-labeled oligonucleotide probes

containing NF- $\kappa$ B elements (approximately 50,000 cpm). These mixtures were incubated for 15 min at room temperature. The DNA protein complexes were separated on a 4% polyacrylamide gel and visualized by autoradiography. To examine the specificity of the NF- $\kappa$ B element probes, we preincubated unlabeled competitor oligonucleotides with nuclear extracts for 15 min before incubation with probes. The probes or competitors used were prepared by annealing the sense and antisense synthetic oligonucleotides as follows: NF- $\kappa$ B site of the *ICAM-1* gene, 5'-tcgaTAGCTTGGAAATTCCGGAGC-3'; NF- $\kappa$ B site of the *IL-2R  $\alpha$  chain* gene, 5'-gatcCGGCAGGGGAATCTCCCTCTC-3'; and AP-1 element of the *IL-8* gene, 5'-gatcGTGATGACTCAGGTT-3'. Underlined sequences represent the NF- $\kappa$ B or AP-1 binding sites. To identify NF- $\kappa$ B proteins in the DNA protein complex revealed by EMSA, we used antibodies specific for various NF- $\kappa$ B family proteins, including p65, p50, c-Rel and p52 (Santa Cruz Biotechnology, Santa Cruz, CA), to elicit a supershift DNA protein complex formation. These antibodies were incubated with the nuclear extracts for 45 min at room temperature before incubation with radio-labeled probes.

#### Results

##### *Expression of CD30, CD30L, ICAM-1 and LFA-1 in normal human lymphocytes and HL cell lines*

To determine whether the expression of ICAM-1 or CD30 is deregulated in HL cell lines, we examined mRNA levels of CD30, CD30L and ICAM-1 in normal PBL and HL cell lines. As shown in Figure 1a, specific amplified CD30 and ICAM-1 products were detected clearly in all 4 HL cell lines. Conversely, amplified bands for CD30L were never detected in HL cell lines. Next, we examined expression of these genes in resting and activated PBL. The detection of an amplified band specific for CD30 was restricted to *in vitro*-activated PBL (PHA-blast). Low levels of ICAM-1 mRNA were found in resting PBL by RT-PCR, and ICAM-1 transcripts were upregulated after activation by PHA. CD30L transcripts were also detected faintly in resting PBL. They were not upregulated after activation by PHA.

To confirm the results of the RT-PCR analysis, we studied the cell surface expression of CD30 and ICAM-1 in normal PBL and HL cell lines by flow cytometry. Consistent with the RT-PCR analysis, strong expression of CD30 (L428: 99.7%; KM-H2: 99.9%; HDLM-2: 99.2%; L540: 98.5%) and ICAM-1 (L428: 97.2%; KM-H2: 98.7%; HDLM-2: 99.4%; L540: 30.1%) was demonstrated in all HL-cell lines (Fig. 1c). Surface CD30 was expressed by activated (20.8–40.2%), but not resting PBL (0.5–1.3%) (Fig. 1c). CD30 expression was less prominent in PHA-blast compared to HL cell lines. Low levels of surface-expressed ICAM-1 protein (6.6–11.8%) were found in resting PBL by flow cytometry. Activation by PHA resulted in the induction of surface ICAM-1 on about 80% of activated PBL (Fig. 1b). Thus, HL cell lines displayed coordinately expressed CD30 and ICAM-1 at mRNA and protein levels.

The surface expression of LFA-1, the major counter-ligand of ICAM-1 in lymphoid cells,<sup>37</sup> was also studied in parallel using a monoclonal antibody against a heavy chain unique to LFA-1 (CD11a). Constitutive expression of LFA-1 was detected in resting as well as in activated PBL (Fig. 1b). In the case of HL cell lines, however, the expression of LFA-1 was strongly depressed (Fig. 1c).

##### *CD30 induces ICAM-1 expression*

RT-PCR and flow cytometry data suggested a close relationship between CD30 and ICAM-1 expression. Ligand-ligated CD30 induces the expression of surface ICAM-1<sup>28</sup> and overexpressed CD30 recently seems to transduce signals independent of CD30L in H/RS cells.<sup>28</sup> To determine the molecular mechanisms of ICAM-1 expression in H/RS cells, we investigated whether CD30 increased the expression of *ICAM-1* gene. For this purpose,



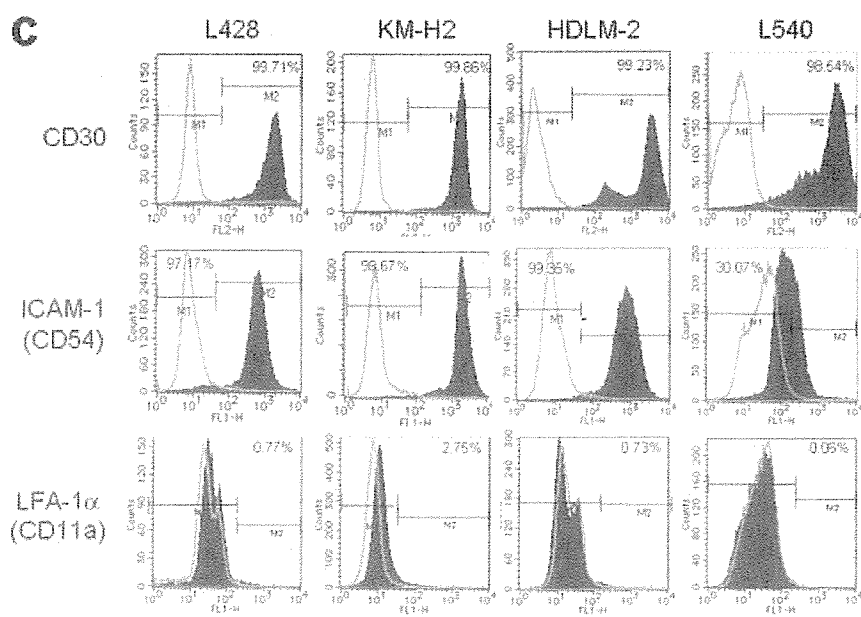
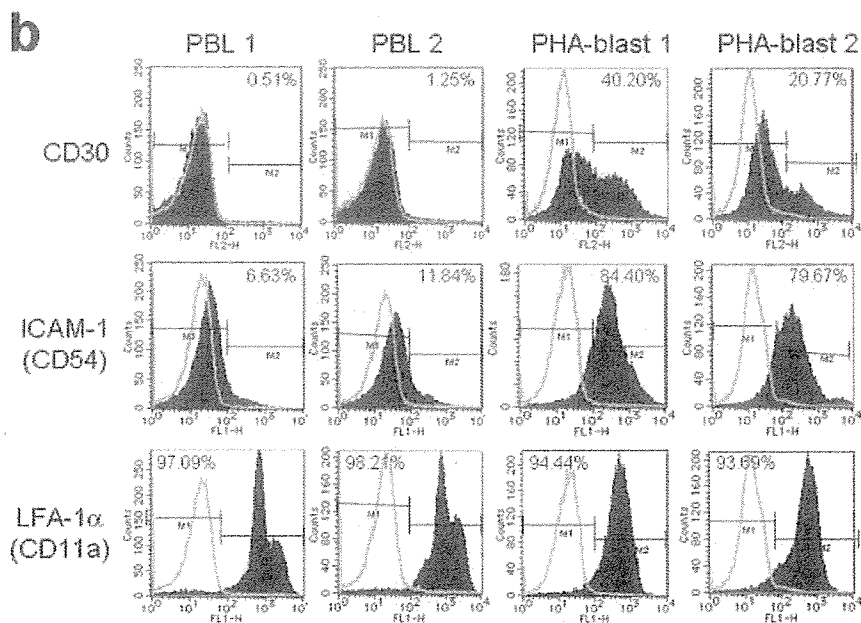
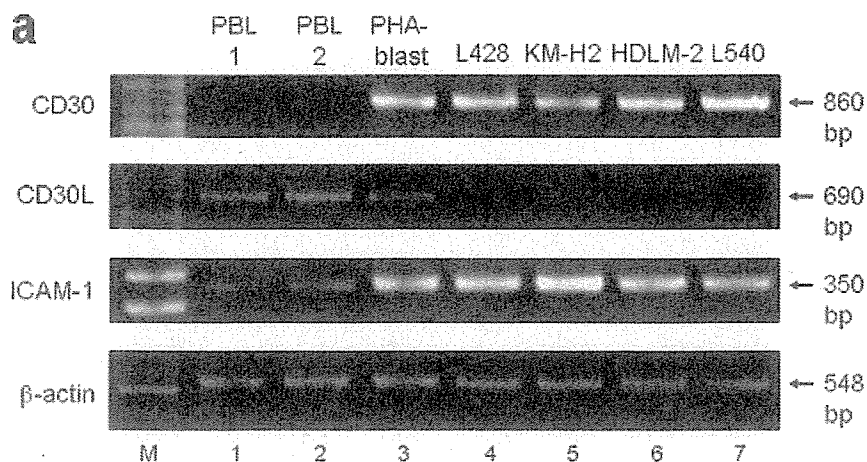
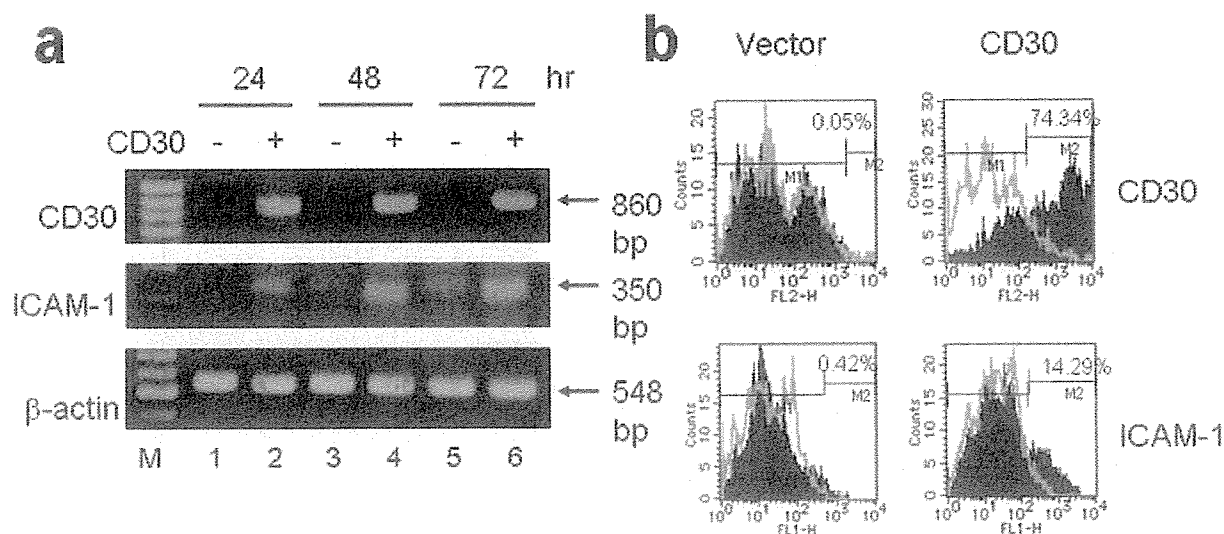


FIGURE 1 – Expression of CD30, CD30L, ICAM-1 and LFA-1 in normal PBL and HL cell lines. (a) Expression of CD30, CD30L and ICAM-1 in cells as assessed by RT-PCR. RNA was prepared from the indicated cells. β-actin expression served as the control. Flow cytometric analysis was carried out on surface expression of CD30, ICAM-1 and LFA-1 α chain in normal PBL (b) and HL cell lines (c). Cells were stained with PE- or FITC-labeled monoclonal antibodies.



**FIGURE 2** – CD30 induces transcription and surface expression of ICAM-1. (a) Total RNA was isolated from 293T cells transfected with an empty pME18S or CD30 expression vector (10  $\mu$ g). The expression of CD30 and ICAM-1 in the RNA extracted at 24–72 hr after transfection, was analyzed by RT-PCR analysis.  $\beta$ -actin served as an internal control in the RT-PCR procedure. (b) Flow cytometric analysis of ICAM-1 induction by CD30 in 293T cells. At 72 hr after transfection of 293T cells with pME18S control plasmid (left panel) or CD30 construct (right panel) (10  $\mu$ g), the viable cells were stained for expression of CD30 with PE-labeled antibody (top panel) and for expression of ICAM-1 with FITC-labeled antibody (bottom panel).

ICAM-1 and CD30 mRNA levels were determined by RT-PCR in 293T cells, which transiently express CD30. As shown in Figure 2a, in the CD30-expressing cell line, ICAM-1 transcript levels were significantly induced compared to the corresponding vector control. These results indicate that CD30 itself is capable of increasing the expression of the *ICAM-1* gene in 293T cells. Furthermore, we measured the surface expression of ICAM-1 on 293T cells transfected with CD30 by flow cytometry. The 4 panels shown in Figure 2b represent the histogram profiles of the CD30 staining (top panel) and ICAM-1 staining (bottom panel) observed in the transfected 293T cells. Approximately 70% of the cells transfected with CD30 expression plasmid were stained with anti-CD30 antibody. Surface ICAM-1 was negative in vector-transfected 293T cells (0.4%). As shown in Figure 2b, the fraction of cells expressing ICAM-1 appeared increased (14%). Thus, consistent with the ability of CD30 to induce transcription of the *ICAM-1* gene, the surface expression of ICAM-1 was induced by CD30.

#### CD30 transactivation of the *ICAM-1* promoter

To confirm that CD30-induced ICAM-1 upregulation occurred by activating gene transcription, the *ICAM-1* 5'-flanking region was analyzed with promoter/reporter gene constructs. 293T cells were transiently transfected with a reporter gene construct containing the -1353 nucleotides of the *ICAM-1* upstream regulatory sequences (pBHluc1.3). Coexpression of CD30 caused 6-fold elevation in the activity of this *ICAM-1*-driven reporter construct in 293T cells, whereas the negative-control vector, pBHlucOL1 showed only low background activity (Fig. 3a), suggesting that CD30 activates *ICAM-1* gene at the transcriptional level.

To locate the *cis*-regulatory element(s) present within the 5'-flanking sequence of the *ICAM-1* promoter that confers CD30 responsiveness, we transfected a series of pBHluc1.3 mutants within 5' deletions of various lengths (the largest mutant beginning at bp -941 and the smallest beginning at bp -136) into 293T cells (Fig. 3a). High levels of induction were observed with the reporter constructs containing *ICAM-1* 5'-flanking sequence starting with position -1353 (pBHluc1.3) to position -353 (construct D). Further deletion to -136 (construct E) resulted in a complete loss of CD30-induced promoter activity. It was apparent

that the *ICAM-1* 5'-flanking sequence between -353 and -136 was required for the promoter to respond to CD30.

Sequence analysis of the CD30-responsive region between -353 and -136 showed potential binding sites for 5 transcription factors: AP-1 (-284 to -278), Sp1 (-206 to -201), C/EBP (-199 to -196), Ets (-153 to -150) and NF- $\kappa$ B (-187 to -178). Hou *et al.*<sup>39</sup> and Ledebur and Parks<sup>35</sup> demonstrated that TNF- $\alpha$ -induced activation of the *ICAM-1* promoter required the NF- $\kappa$ B site. To determine the functional importance of the NF- $\kappa$ B site, transfections with mutant *ICAM-1* promoter/luciferase reporter gene constructs with specific mutations in either the NF- $\kappa$ B (designated pGL1.3 $\kappa$ B-) or the Ets (designated pGL1.3Ets-) binding site<sup>33</sup> were carried out (Fig. 3b). Mutation of the NF- $\kappa$ B site in the *ICAM-1* promoter reduced significantly CD30-mediated luciferase activity in 293T cells, whereas the Ets site mutation had no effect. These experiments indicated that the response to CD30 stimulation required an intact binding site for NF- $\kappa$ B.

#### Dominant interfering components of the NF- $\kappa$ B pathway inhibit CD30-mediated transactivation of *ICAM-1* gene expression

CD30 signals that induce NF- $\kappa$ B activation have been intensively investigated.<sup>24–27</sup> Activation of NF- $\kappa$ B requires phosphorylation of 2 conserved serine residues of I $\kappa$ B $\alpha$  (Ser-32 and Ser-36) and I $\kappa$ B $\beta$  (Ser-19 and Ser-23) within their N-terminal domains.<sup>40</sup> Phosphorylation leads to ubiquitination and the 26S proteasome-mediated degradation of I $\kappa$ B, thereby releasing NF- $\kappa$ B from the complex to translocate to the nucleus and activate genes.<sup>40</sup> The high-molecular weight complex, IKK complex, which is composed of 2 catalytic subunits, IKK $\alpha$  and IKK $\beta$ , and a regulatory subunit, IKK $\gamma$ , phosphorylates I $\kappa$ B.<sup>41</sup> Recent studies indicated that members of the mitogen-activated protein kinase kinase protein kinase family mediate physiologic activation of IKK.<sup>42</sup> These kinases include NIK<sup>43</sup> and mitogen-activated protein kinase/extracellular signal-regulated kinase 1.<sup>44</sup> As discussed above, NF- $\kappa$ B activation by ligand-ligated CD30 is likely to be mediated by recruitment of downstream signal-transducing molecule TRAF proteins, TRAF2 and TRAF5,<sup>24–27</sup> and activates the NIK-IKK-NF- $\kappa$ B pathway (Fig. 4, left panel).<sup>45</sup> We therefore examined whether CD30-mediated transactivation of *ICAM-1*

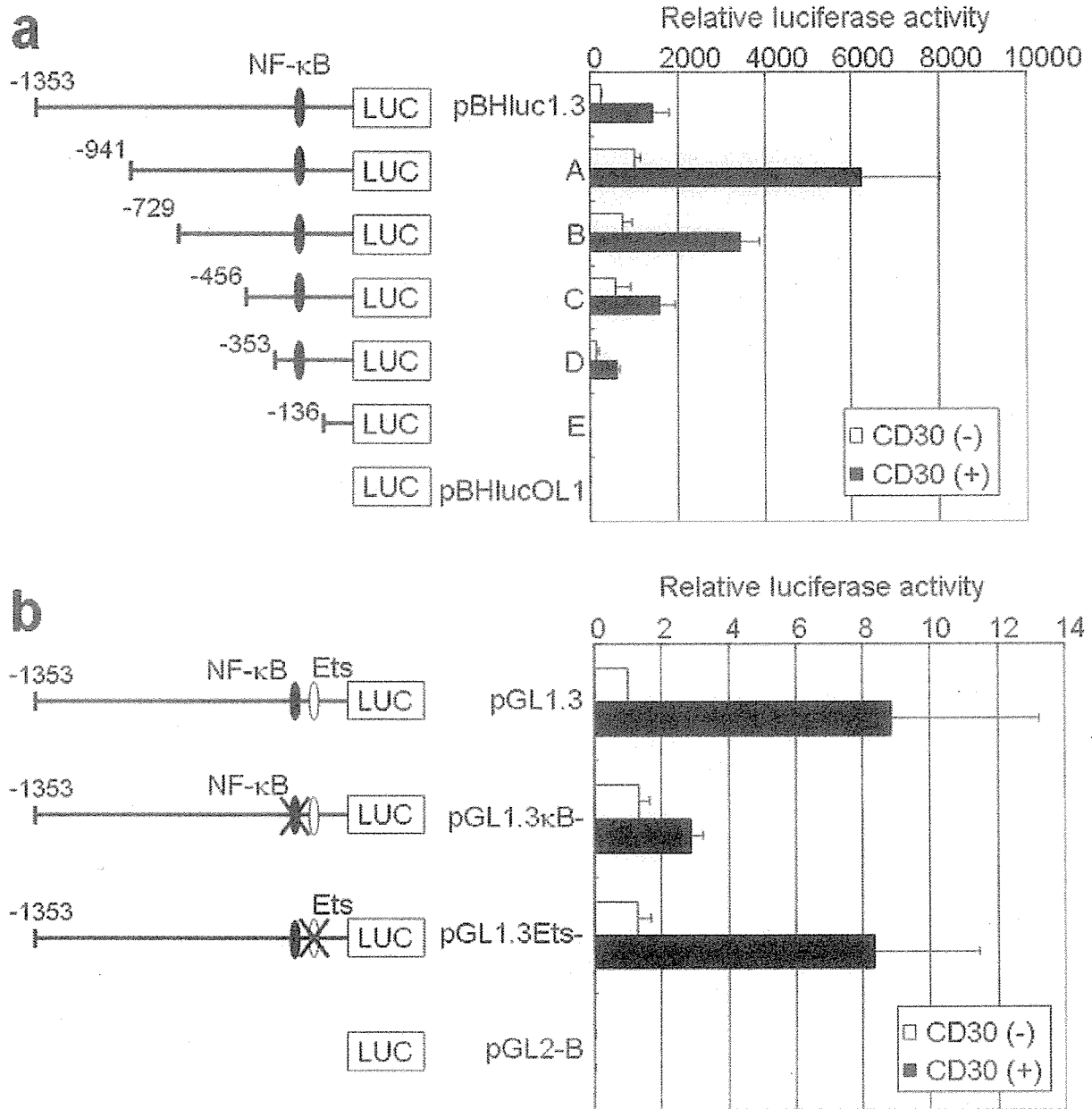


**FIGURE 3** – Identification of a critical CD30-responsive region of the ICAM-1 promoter. (a) Deletion analysis of the *cis*-elements required for CD30-induced ICAM-1 promoter activity. A series of constructs of 5'-deletion mutants and a fusion construct linked to the luciferase gene (LUC) were tested for transcriptional activity after transfection into 293T cells. The endpoints of fragments are indicated relative to the transcription start site. Luciferase reporter constructs (0.2  $\mu$ g) were cotransfected with pME18S (-CD30) or pME-hCD30 (+CD30) (2  $\mu$ g) into 293T cells. pRL-TK (0.004  $\mu$ g) was also cotransfected as an internal control plasmid. Open and solid bars represent luciferase activity of pME18S and pME-hCD30-transfected cells, respectively. The activities are expressed relative to that of cells transfected with pBHlucOL1 and pME18S, which was defined as one. Data are mean  $\pm$  SD values of 3 independent experiments. (b) Mutation of the NF- $\kappa$ B site suppresses CD30-induced ICAM-1 promoter activity. All constructs were transfected into 293T cells with pME18S and pME-hCD30. The activities are expressed relative to that of cells transfected with pGL1.3 and pME18S, which was defined as one.

gene expression involves signal transduction components in NF- $\kappa$ B activation. I $\kappa$ B $\alpha$  $\Delta$ N<sup>29</sup> and I $\kappa$ B $\beta$  $\Delta$ N<sup>30</sup> lacking the N-terminal region can be neither phosphorylated nor ubiquitinated. Because both mutants can still interact with NF- $\kappa$ B, they are very potent inhibitors of its activity by keeping it permanently in the cytoplasm. Dominant negative forms of the NIK and IKK, which are

created by mutations in the kinase activation domain, are capable of blocking phosphorylation of IKK and I $\kappa$ B, respectively.<sup>31</sup> N-terminal truncated TRAF2 and TRAF5 mutants that lack ring finger and zinc finger domains inhibit NF- $\kappa$ B activation, because the zinc finger domain is required for NF- $\kappa$ B activation.<sup>26</sup> These dominant interfering mutants of I $\kappa$ B $\alpha$ , I $\kappa$ B $\beta$ , TRAF2 and TRAF5 and

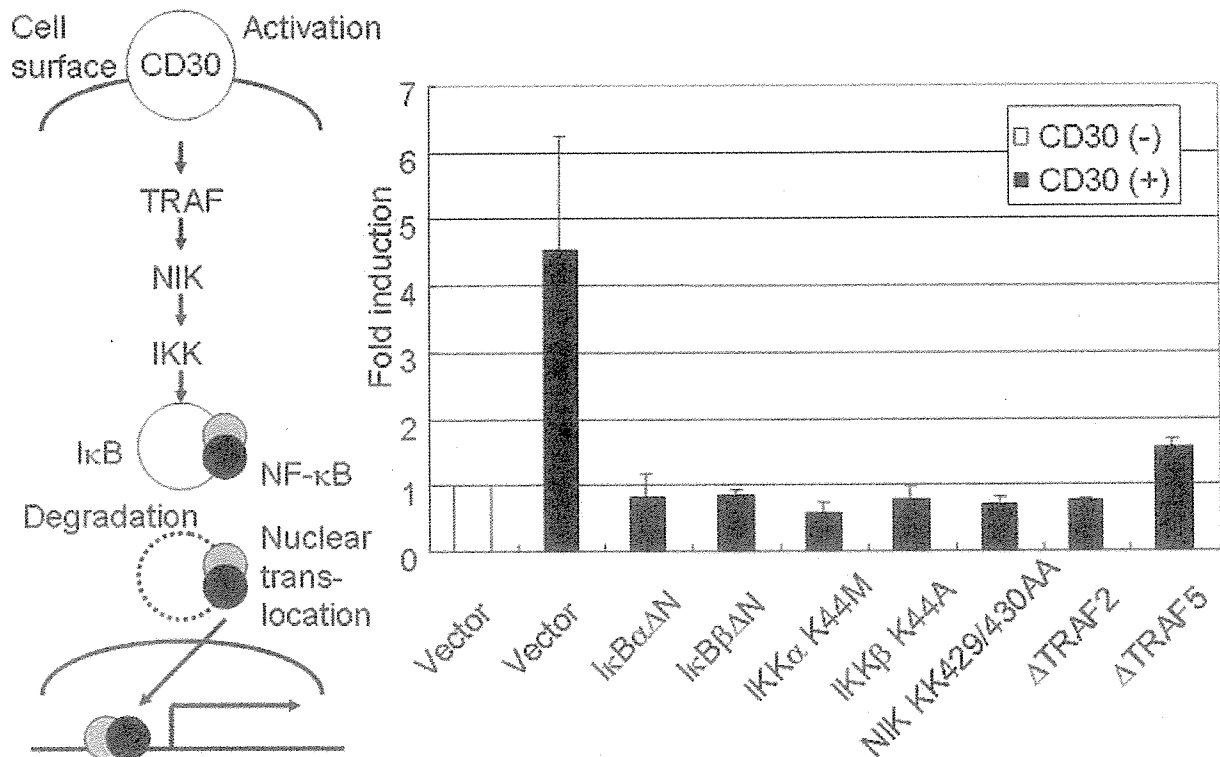


**FIGURE 4** – CD30 transactivates the ICAM-1 promoter mainly through the NF- $\kappa$ B pathway. Functional effects of I $\kappa$ B $\alpha$ , I $\kappa$ B $\beta$ , TRAF2 and TRAF5 dominant interfering mutants and kinase-deficient IKK $\alpha$ , IKK $\beta$  and NIK mutants on CD30-induced activation of the ICAM-1 promoter. The indicated effector plasmids (1  $\mu$ g) were cotransfected with pGL1.3 (0.2  $\mu$ g) into 293T cells. The open bar represents luciferase activity of empty vector (pCMV4) without CD30. Solid bars represent luciferase activity of I $\kappa$ B $\alpha$ , I $\kappa$ B $\beta$ , TRAF2 and TRAF5 mutants and kinase-deficient IKK $\alpha$ , IKK $\beta$  and NIK mutants in the presence of CD30. The activities are given relative to the activity of empty vector (pCMV4) without CD30, which was defined as one. Data are mean  $\pm$  SD values of 3 independent experiments. The *left panel* shows molecules involved in CD30-mediated NF- $\kappa$ B activation.

kinase-deficient mutants of IKK $\alpha$ , IKK $\beta$  and NIK were tested for their ability to inhibit CD30-mediated activation of an ICAM-1-driven reporter gene. Expression of these various inhibitory mutants inhibited induction of the ICAM-1 promoter activation by CD30 (Fig. 4). These data demonstrate that signalling components, TRAF2, TRAF5, NIK and IKK, involved in the activation of NF- $\kappa$ B, are necessary for CD30 transactivation of the ICAM-1 promoter.

#### C-terminal region of CD30 activates ICAM-1 promoter

A region of approximately 100 amino acids from the C-terminal region of CD30 is involved in NF- $\kappa$ B activation.<sup>24,25,27</sup> Mutation analyses of this region have shown that TRAF2 recognizes D2 and D3 subdomains of CD30. TRAF5 recognizes and binds to the D3 subdomain of CD30. The D1 subdomain is sufficient for NF- $\kappa$ B activation without interaction with TRAF2 or TRAF5 (Fig. 5a).<sup>24–27,45</sup> We investigated which C-terminal region of CD30 plays a role in induction of ICAM-1. As shown in Figure 5b, ICAM-1-driven reporter gene activity was not increased by CD30 $\Delta$ 95, which lacks the C-terminal region of CD30. Activation of this reporter was observed with CD30 wild-type. The C-terminal region of CD30 seems to be required for activation of the ICAM-1 promoter. CD30 $\Delta$ 95 has been reported to inhibit recruitment of TRAF proteins and abrogate downstream activation of NF- $\kappa$ B in HL cell lines.<sup>28</sup> We determined if ICAM-1 activation by CD30 overexpression would be inhibited by expression of a CD30 mutant lacking the TRAF binding domain by reporter gene analysis using the ICAM-1-driven luciferase construct. As expected, the

CD30 mutant inhibited constitutive ICAM-1 activation in an HL cell line, L428 (Fig. 5c, *left panel*). Similar results were obtained in transfected KM-H2 and HDLM-2 (Fig. 5c, *right panel*). These results indicate that expression of the CD30 mutant without the C-terminal tail can inhibit recruitment of TRAF proteins, abrogate activation of NF- $\kappa$ B, and inhibit downstream activation of ICAM-1.

#### CD30 induces binding of NF- $\kappa$ B family proteins to the NF- $\kappa$ B element of the ICAM-1 promoter

Because the mutational analyses of the ICAM-1 promoter indicated that CD30 activated transcription through the NF- $\kappa$ B binding site, it was important to identify the nuclear factors that bind to this site. We investigated the induction and binding of nuclear factors to NF- $\kappa$ B binding sequences in the ICAM-1 promoter region by transfection with CD30. As shown in Figure 6a, a complex formed with the ICAM-1 NF- $\kappa$ B oligonucleotide probe was induced in 293T cells transfected with CD30. This binding activity was reduced by the addition of cold probe and the *IL-2R*  $\alpha$  chain gene NF- $\kappa$ B binding site but not by an oligonucleotide containing the AP-1 binding site (Fig. 6b, *lanes 2–4*). We characterized the CD30-induced complex identified by the ICAM-1 NF- $\kappa$ B probe. This complex was supershifted or reduced by the addition of anti-p50 or anti-p65 antibody (Fig. 6b, *lanes 5–8*), suggesting that CD30-induced ICAM-1 NF- $\kappa$ B binding activity is composed of p50 and p65. Therefore, CD30 induces ICAM-1 gene expression, at least in part, through the induced binding of p50 and p65 to NF- $\kappa$ B site in the ICAM-1 promoter region.

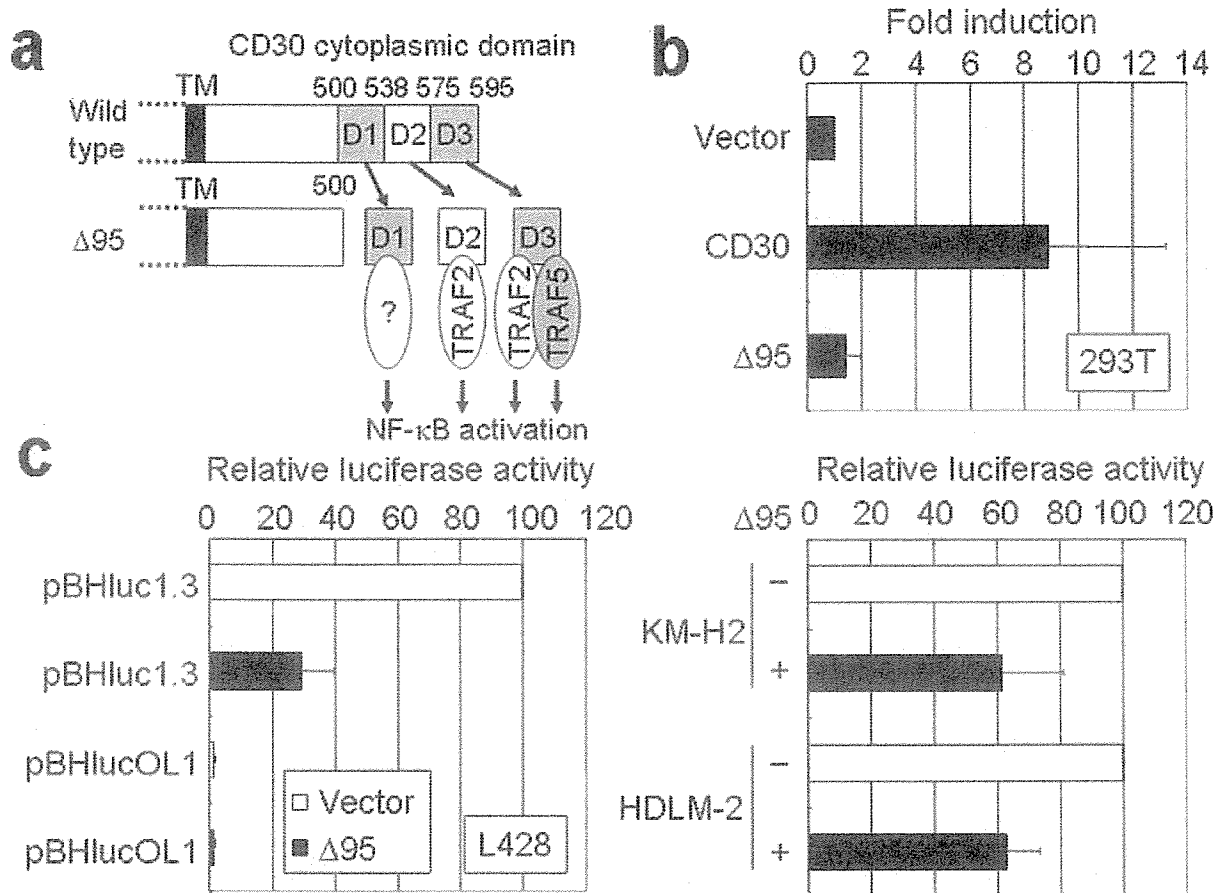


**FIGURE 5** – The C-terminal domain of CD30 is required for its activity. (a) Schematic diagrams of wild-type and mutant CD30 protein. TM, transmembrane domain. (b) Induction of ICAM-1 transcriptional activity by wild-type CD30 and CD30 deletion mutant. 293T cells were transfected with wild-type and CD30 mutant (2  $\mu$ g each) and a luciferase reporter construct (pBHLuc1.3; 0.2  $\mu$ g) to identify the C-terminal region essential for its function. pRL-TK (0.004  $\mu$ g) was also cotransfected as an internal control plasmid. A negative control vector pME18S, a wild-type pME-hCD30 and CD30 $\Delta$ 95 are shown as vector, CD30 and  $\Delta$ 95 on the abscissa, respectively. The results are expressed as fold induction relative to the basal level measured in cells transfected with pME18S. Data represent mean  $\pm$  SD of 3 separate experiments. (c) Suppression of constitutive ICAM-1 activity by transduction of CD30 mutant in HL cell lines. pBHLuc1.3 or pBHLucOL1 was transiently transfected along with an empty vector or mutant CD30 construct. The activities are expressed relative to that of cells transfected with pBHLuc1.3 and an empty vector, which was defined as 100. Values represent mean  $\pm$  SD of 3 separate experiments.

#### Binding of NF- $\kappa$ B family proteins to the CD30-responsive element within the ICAM-1 upstream regulatory sequences in HL cell lines

Because we have shown that HL cell lines constitutively express ICAM-1 mRNA and surface ICAM-1 protein, we sought to determine whether HL cell lines exhibited increased NF- $\kappa$ B DNA binding activity. Using the NF- $\kappa$ B-like region derived from the ICAM-1 promoter as probes in EMSA, we observed clear shifted bands when these probes were incubated with nuclear extracts from all HL cell lines (Fig. 6c, lanes 1,4,7,10). These shifted complexes were specific to the NF- $\kappa$ B sequence because complex formations were reduced by the addition of excess cold probe but not by an oligonucleotide containing the AP-1 binding site (Fig. 6c, lanes 2,3,5,6,8,9,11,12). To determine the subunit composition of NF- $\kappa$ B complex, we used a specific antibody to induce a supershift. In KM-H2 cells, anti-p50 and anti-p65 antibodies caused supershifting or reduction in the NF- $\kappa$ B complex (Fig. 6c, lanes 13,14). These results indicate that the augmented NF- $\kappa$ B binding activity may play a key role in the observed activation of ICAM-1 gene in HL cell lines. Of note, L540 cells, in which surface ICAM-1 is expressed more weakly than in other HL

cell lines, exhibited NF- $\kappa$ B binding activity more weakly than other HL cell lines did, suggesting that a direct correlation between the levels of surface ICAM-1 expression and NF- $\kappa$ B binding activity among HL cell lines. Thus, HL cell lines express constitutively the ICAM-1 gene, at least in part, through the induced binding of p50 and p65 NF- $\kappa$ B family members to the NF- $\kappa$ B element of the ICAM-1 promoter, and this effect is at least in part dependent on CD30.

#### Discussion

ICAM-1 is the counter receptor for LFA-1.<sup>6</sup> The LFA-1/ICAM-1 pair serves as major adherence receptor required for intercellular interaction and communication of immune contact cells.<sup>46,47</sup> It has been reported that CD30 stimulation induces homotypic cell aggregation of human lymphoma line.<sup>48</sup> It has been reported recently that CD30 signals strongly upregulate ICAM-1 expression and increase ICAM-1-dependent cell clustering of lymphocytes in normal activated murine lymph node cells.<sup>58</sup> Constitutively expressed ICAM-1 is a characteristic feature of H/RS cells in lymph node biopsy samples from patients with HL.<sup>7</sup> Tissue

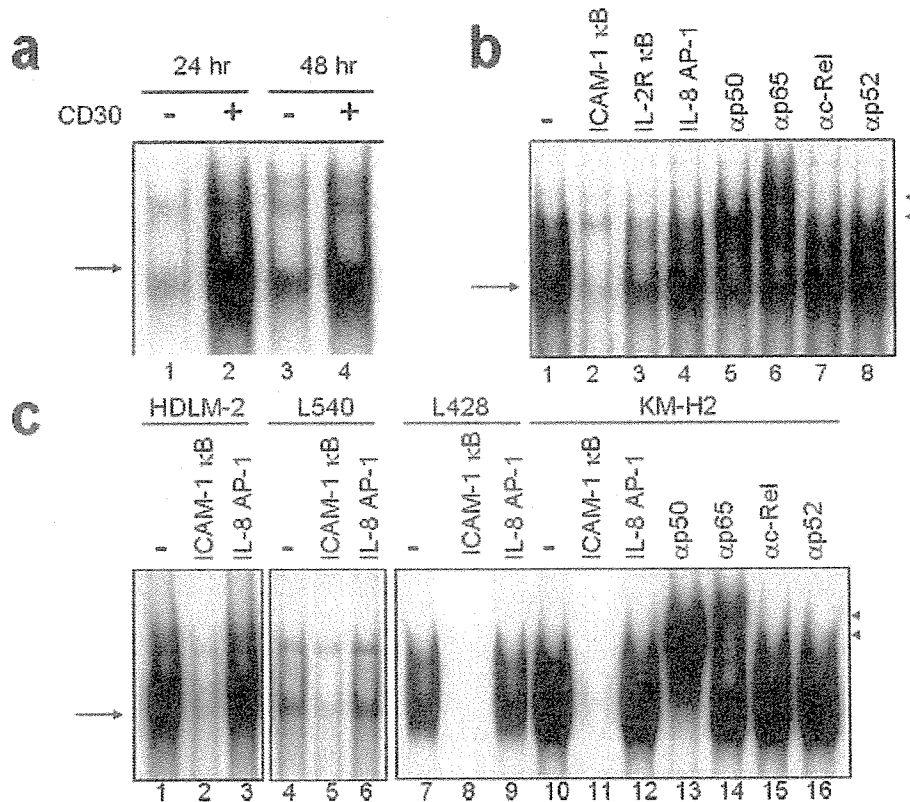


**FIGURE 6** – CD30-dependent binding of NF- $\kappa$ B family proteins to the CD30-responsive elements. (a) NF- $\kappa$ B activation in 293T cells transfected with CD30 expression vector evaluated by EMSA. Nuclear extracts prepared at the indicated time points from 293T cells, transfected with pME18S or pME-hCD30 (10  $\mu$ g), were mixed with ICAM-1 NF- $\kappa$ B [ $^{32}$ P]-labeled probe. (b) Sequence specificity of NF- $\kappa$ B binding activity and characterization of NF- $\kappa$ B proteins that bound to the NF- $\kappa$ B binding site of the *ICAM-1* gene. Competition assays were carried out with nuclear extracts from 293T cells transfected with CD30 expression vector. Where indicated, 100-fold excess amounts of each specific competitor oligonucleotide (lanes 2–4) were added to the reaction mixture with labeled probe. Supershift assay of NF- $\kappa$ B DNA binding complex in the same nuclear extracts was also carried out. Where indicated, appropriate antibodies were added to the reaction mixture (lanes 5–8). (c) Binding of nuclear proteins from HL cell lines to the ICAM-1 NF- $\kappa$ B probe. Nuclear extracts were incubated with labeled probe. Competition assays were carried out using nuclear extracts from HDLM-2 (lanes 1–3), L540 (lanes 4–6), L428 (lanes 7–9) and KM-H2 (lanes 10–12) cells. Where indicated, 100-fold excess amounts of each specific competitor oligonucleotide (lanes 2,3,5,6,8,9,11,12) were added to the reaction mixture with labeled probe. Supershift assay of NF- $\kappa$ B DNA binding complex in nuclear extracts from KM-H2 cells was also carried out. Where indicated, appropriate antibodies were added to the reaction mixture (lanes 13–16).

ICAM-1 overexpression associates with increased serum levels of soluble ICAM-1 in HL.<sup>9</sup> We examined the expression of ICAM-1 and LFA-1 in 4 HL cell lines. In sharp contrast to an undetectable level of LFA-1, strong induction of ICAM-1 was seen in all HL cell lines. Interestingly, all cell lines showed striking upregulation of CD30 expression, but lacked expression of CD30L. It is unlikely that the LFA-1/ICAM-1 pathway mediated the homotypic cell-cell interaction of HL-cell lines and induced ICAM-1 expression through binding of CD30L to CD30.

In our present study, we demonstrated that constitutive ICAM-1 expression in HL cell lines is driven by ligand-independent NF- $\kappa$ B signalling from overexpressed CD30. This conclusion is based on the observations that: (i) ICAM-1 is overexpressed in 293T cells transfected with a CD30 expression plasmid; (ii) inhibition of the TRAF/NF- $\kappa$ B pathway effectively suppresses the CD30-mediated transactivation of *ICAM-1* gene expression; (iii) the NF- $\kappa$ B binding site in the promoter region of ICAM-1 is critically involved in activation of the ICAM-1 promoter by CD30; and (iv) coexpression of a CD30 mutant lacking the C-terminal region, which is required for recruitment of TRAF2 and TRAF5, abrogated the ICAM-1 promoter activity. Because CD30L is not expressed in 293T cells (data not shown) and HL cell lines, autocrine or paracrine activation of CD30 is highly unlikely. Consis-

tent with our results, Hinz *et al.*<sup>49</sup> demonstrated that ICAM-1 expression in HL cell lines was regulated by NF- $\kappa$ B using large-scale gene expression profiling. These observations indicate that ligand-independent assembly of overexpressed CD30 in HL cell lines recruits TRAF2 and TRAF5 and consistently triggers downstream signalling. These events result in apparently constitutive, but CD30-dependent activation of ICAM-1 through the NF- $\kappa$ B pathway in HL cell lines.

In addition, deletion constructs A to D suggest that the region between -941 and -353 may also be important for the inductive effect of CD30. Sequence analysis showed the existence of potential binding sites for 2 transcription factors, NF- $\kappa$ B (-500 to -489) and AP-3 (-374 to -355). Further studies will be required, including *in vitro* mutagenesis of proposed regulatory elements, to analyze more precisely the location of diverse controlling elements and their role in *ICAM-1* gene regulation.

Constitutively activated NF- $\kappa$ B is the hallmark of HL cell lines and primary cells.<sup>50</sup> Interestingly, mutation of I $\kappa$ B $\alpha$ , producing non-functional or unstable I $\kappa$ B $\alpha$  proteins, has been implicated in aberrant constitutive NF- $\kappa$ B activation in HL cell lines.<sup>51,52</sup> Recent data implicate persistently activated IKK complex as the major cause of constitutive NF- $\kappa$ B activity.<sup>53</sup> Our finding that ICAM-1 activation is blocked by CD30 mutant lacking the C-ter-

minal region in L428 and KM-H2 cells with defective I $\kappa$ B $\alpha$ , indicates that irrespective of the presence or absence of mutations in I $\kappa$ B $\alpha$ , overexpressed CD30 drives ICAM-1 activation through the NF- $\kappa$ B pathway in HL cell lines. These findings demonstrate a previously unrecognized link between 2 well known phenotypic characteristics of HL cell lines, CD30 overexpression and constitutive expression of ICAM-1.

Expression of functional CD30L has been observed on lymphocytes and granulocytes that surrounded H/RS cells in HL-affected lymph nodes.<sup>16,54</sup> It is also possible that other normal tumor-infiltrating cells, such as mast cells, can produce CD30L and thereby stimulate the growth of H/RS cells *via* CD30/CD30L interaction.<sup>55</sup>

In summary, our data demonstrate that in addition to ligand-dependent activation of CD30 signalling, ligand-independent signalling by overexpressed CD30 drives NF- $\kappa$ B activation and this leads to constitutive ICAM-1 expression in HL.

#### Acknowledgements

We thank Dr. C. Stratowa, Dr. T.P. Parks, Dr. D.W. Ballard and Dr. R. Gelezianus for providing expression vectors for ICAM-1 promoter constructs, for deletion mutants of I $\kappa$ B and for the kinase-deficient K44M IKK $\alpha$ , K44A IKK $\beta$  and KK429/430AA NIK mutants.

#### References

- Dorreen MS, Habeshaw JA, Stansfeld AG, Wrigley PF, Lister TA. Characteristics of Sternberg-Reed, and related cells in Hodgkin's disease: an immunohistological study. *Br J Cancer* 1984;49:465-76.
- Gruss H-J, Pinto A, Duyster J, Poppema S, Herrmann F. Hodgkin's disease: a tumor with disturbed immunological pathways. *Immunol Today* 1997;18:156-63.
- Coussens LM, Werb Z. Inflammatory cells and cancer: think different! *J Exp Med* 2001;193:F23-6.
- Carlos TM, Harlan JM. Leukocyte-endothelial adhesion molecules. *Blood* 1994;84:2068-101.
- Simmons D, Makgoba MW, Seed B. ICAM, an adhesion ligand of LFA-1, is homologous to the neural cell adhesion molecule NCAM. *Nature* 1988;331:624-7.
- Marlin SD, Springer TA. Purified intercellular adhesion molecule-1 (ICAM-1) is a ligand for lymphocyte function-associated antigen 1 (LFA-1). *Cell* 1987;51:813-9.
- Ruco LP, Pomponi D, Pigott R, Gearing AJ, Baiocchi A, Baroni CD. Expression and cell distribution of the intercellular adhesion molecule, vascular cell adhesion molecule, endothelial leukocyte adhesion molecule, and endothelial cell adhesion molecule (CD31) in reactive human lymph nodes and in Hodgkin's disease. *Am J Pathol* 1992;140:1337-44.
- Banks RE, Gearing AJ, Hemingway IK, Norfolk DR, Perren TJ, Selby PJ. Circulating intercellular adhesion molecule-1 (ICAM-1), E-selectin and vascular cell adhesion molecule-1 (VCAM-1) in human malignancies. *Br J Cancer* 1993;68:122-4.
- Pizzolo G, Vinante F, Nadali G, Ricetti MM, Morosato L, Marroccella R, Vincenzi C, Semenzato G, Chilosi M. ICAM-1 tissue overexpression associated with increased serum levels of its soluble form in Hodgkin's disease. *Br J Haematol* 1993;84:161-2.
- Christiansen I, Enblad G, Kalkner KM, Gidlöf C, Glimelius B, Totterman TH. Soluble ICAM-1 in Hodgkin's disease: a promising independent predictive marker for survival. *Leuk Lymphoma* 1995;19:243-51.
- Gruss H-J, Dower SK. Tumor necrosis factor ligand superfamily: involvement in the pathology of malignant lymphomas. *Blood* 1995;85:3378-404.
- Falini B, Pileri S, Pizzolo G, Durkop H, Flenghi L, Stürpe F, Martelli MF, Stein H. CD30 (Ki-1) molecule: a new cytokine receptor of the tumor necrosis factor receptor superfamily as a tool for diagnosis and immunotherapy. *Blood* 1995;85:1-14.
- Schwab U, Stein H, Gerdes J, Lemke H, Kirchner H, Schaadt M, Diehl V. Production of a monoclonal antibody specific for Hodgkin and Sternberg-Reed cells of Hodgkin's disease and a subset of normal lymphoid cells. *Nature* 1982;299:65-7.
- Nadali G, Tavecchia L, Zanolin E, Bonfante V, Viviani S, Camerini E, Musto P, Di Renzo N, Carotenuto M, Chilosi M, Krampera M, Pizzolo G. Serum level of the soluble form of the CD30 molecule identifies patients with Hodgkin's disease at high risk of unfavorable outcome. *Blood* 1998;91:3011-6.
- Stein H, Mason DY, Gerdes J, O'Connor N, Wainscoat J, Pallesen G, Gatter K, Falini B, Delso G, Lemke H, Schwarting R, Lennert K. The expression of the Hodgkin's disease associated antigen Ki-1 in reactive and neoplastic lymphoid tissue: evidence that Reed-Sternberg cells and histiocytic malignancies are derived from activated lymphoid cells. *Blood* 1985;66:848-58.
- Pinto A, Aldinucci D, Gioghini A, Zagonel V, Degan M, Improta S, Juzbasic S, Todesco M, Perin V, Gattei V, Herrmann F, Gruss H-J, et al. Human eosinophils express functional CD30 ligand and stimulate proliferation of a Hodgkin's disease cell line. *Blood* 1996;88:3299-305.
- Younes A, Consoli U, Zhao S, Snell V, Thomas E, Gruss H-J, Cabanillas F, Andreeff M. CD30 ligand is expressed on resting normal and malignant human B lymphocytes. *Br J Haematol* 1996;93:569-71.
- Gruss H-J, Boiani N, Williams DE, Armitage RJ, Smith CA, Goodwin RG. Pleiotropic effects of the CD30 ligand on CD30-expressing cells and lymphoma cell lines. *Blood* 1994;83:2045-56.
- Masuda M, Ishida C, Arai Y, Okamura T, Ohsawa M, Shimakage M, Mizoguchi H. Dual action of CD30 antigen: anti-CD30 antibody induced apoptosis and interleukin-8 secretion in Ki-1 lymphoma cells. *Int J Hematol* 1998;67:257-65.
- Leca G, Vita N, Maiza H, Fasseu M, Bensussan A. A monoclonal antibody to the Hodgkin's disease-associated antigen CD30 induces activation and long-term growth of human autoreactive  $\gamma\delta$  T cell clone. *Cell Immunol* 1994;156:230-9.
- McDonald PP, Cassatella MA, Bald A, Maggi E, Romagnani S, Gruss H-J, Pizzolo G. CD30 ligation induces nuclear factor- $\kappa$ B activation in human T cell lines. *Eur J Immunol* 1995;25:2870-6.
- Bowen MA, Lee RK, Miragliotta G, Nam SY, Podack ER. Structure and expression of murine CD30 and its role in cytokine production. *J Immunol* 1996;156:442-9.
- Baker SJ, Reddy EP. Modulation of life and death by the TNF receptor superfamily. *Oncogene* 1998;17:3261-70.
- Gedrich RW, Gilfillan MC, Duckett CS, Van Dongen JL, Thompson CB. CD30 contains two binding sites with different specificities for members of the tumor necrosis factor receptor-associated factor family of signal transducing proteins. *J Biol Chem* 1996;271:12852-8.
- Lee SY, Lee SY, Kandala G, Liou M-L, Liou H-C, Choi Y. CD30/TNF receptor-associated factor interaction: NF- $\kappa$ B activation and binding specificity. *Proc Natl Acad Sci USA* 1996;93:9699-9703.
- Aizawa S, Nakano H, Ishida T, Horie R, Nagai M, Ito K, Yagita H, Okumura K, Inoue J, Watanabe T. Tumor necrosis factor receptor-associated factor (TRAF) 5 and TRAF2 are involved in CD30-mediated NF $\kappa$ B activation. *J Biol Chem* 1997;272:2042-5.
- Horie R, Aizawa S, Nagai M, Ito K, Higashihara M, Ishida T, Inoue J, Watanabe T. A novel domain in the CD30 cytoplasmic tail mediates NF $\kappa$ B activation. *Int Immunol* 1998;10:203-10.
- Horie R, Watanabe T, Morishita Y, Ito K, Ishida T, Kanegae Y, Saito I, Higashihara M, Mori S, Kadin ME, Watanabe T. Ligand-independent signaling by overexpressed CD30 drives NF- $\kappa$ B activation in Hodgkin-Reed-Sternberg cells. *Oncogene* 2002;21:2493-503.
- Brockman JA, Scherer DC, McKinsey TA, Hall SM, Qi X, Lee WY, Ballard DW. Coupling of a signal response domain in I $\kappa$ B $\alpha$  to multiple pathways for NF- $\kappa$ B activation. *Mol Cell Biol* 1995;15:2809-18.
- McKinsey TA, Brockman JA, Scherer DC, Al-Murrani SW, Green PL, Ballard DW. Inactivation of I $\kappa$ B $\beta$  by the tax protein of human T-cell leukemia virus type 1: a potential mechanism for constitutive induction of NF- $\kappa$ B. *Mol Cell Biol* 1996;16:2083-90.
- Gelezianus R, Ferrell S, Lin X, Mu Y, Cunningham ET Jr, Grant M, Connelly MA, Hambor JE, Marcu KB, Greene WC. Human T-cell leukemia virus type 1 Tax induction of NF- $\kappa$ B involves activation of the I $\kappa$ B kinase  $\alpha$  (IKK $\alpha$ ) and IKK $\beta$  cellular kinases. *Mol Cell Biol* 1998;18:5157-65.
- Voraberger G, Schafer R, Stratowa C. Cloning of the human gene for intercellular adhesion molecule 1 and analysis of its 5'-regulatory region. Induction by cytokines and phorbol ester. *J Immunol* 1991;147:2777-86.
- Ledeber HC, Parks TP. Transcriptional regulation of the intercellular adhesion molecule-1 gene by inflammatory cytokines in human endothelial cells. Essential roles of a variant NF- $\kappa$ B site and p65 homodimers. *J Biol Chem* 1995;270:933-43.
- Gattei V, Degan M, Gioghini A, De Julis A, Improta S, Rossi FM, Aldinucci D, Perin V, Serraino D, Babare R, Zagonel V, Gruss H-J, et al. CD30 ligand is frequently expressed in human hematopoietic malignancies of myeloid and lymphoid origin. *Blood* 1997;89:2048-59.
- Anai T, Yamamoto E, Awano S, Yu W, Turner AJ, Takehara T. Effects of periodontopathic bacteria on the expression of endothelin-1 in gingival epithelial cells in adult periodontitis. *Clin Sci* 2002;103:327S-31S.

36. Mori N, Fujii M, Ikeda S, Yamada Y, Tomonaga M, Ballard DW, Yamamoto N. Constitutive activation of NF- $\kappa$ B in primary adult T-cell leukemia cells. *Blood* 1999;93:2360-8.
37. Springer TA. Adhesion receptors of the immune system. *Nature* 1990;346:425-34.
38. Nam S-Y, Cho K-S, Heo Y-M, Ha J-C, Kim Y-H, Keun YK, Han Hwang P, Kim H-M, Podack ER. Regulation of lymphocyte clustering by CD30-mediated ICAM-1 up-regulation. *Cell Immunol* 2002;219:38-47.
39. Hou J, Baichwal V, Cao Z. Regulatory elements and transcription factors controlling basal and cytokine-induced expression of the gene encoding intercellular adhesion molecule 1. *Proc Natl Acad Sci USA* 1994;91:11641-5.
40. Ghosh S, May MJ, Kopp EB. NF- $\kappa$ B and Rel proteins: evolutionarily conserved mediators of immune responses. *Annu Rev Immunol* 2000;16:225-60.
41. Karin M, Ben-Neriah Y. Phosphorylation meets ubiquitination: the control of NF- $\kappa$ B activity. *Annu Rev Immunol* 2000;18:621-63.
42. Zandi E, Karin M. Bridging the gap: composition, regulation, and physiological function of the I $\kappa$ B kinase complex. *Mol Cell Biol* 1999;19:4547-51.
43. Woronicz JD, Gao X, Cao Z, Rothe M, Goeddel DV. I $\kappa$ B kinase- $\beta$ : NF- $\kappa$ B activation and complex formation with I $\kappa$ B kinase- $\alpha$  and NIK. *Science* 1997;278:866-9.
44. Lee FS, Peters RT, Dang LC, Maniatis T. MEKK1 activates both I $\kappa$ B kinase  $\alpha$  and I $\kappa$ B kinase  $\beta$ . *Proc Natl Acad Sci USA* 1998;95:9319-24.
45. Horie R, Higashihara M, Watanabe T. Hodgkin's lymphoma and CD30 signal transduction. *Int J Hematol* 2003;77:37-47.
46. Dougherty GJ, Hogg N. The role of monocyte lymphocyte function-associated antigen 1 (LFA-1) in accessory cell function. *Eur J Immunol* 1987;17:943-7.
47. Wang P, Vanky F, Li SL, Patarroyo M, Klein E. Functional characteristics of the intercellular adhesion molecule-1 (CD54) expressed on cytotoxic human blood lymphocytes. *Cell Immunol* 1990;131:366-80.
48. Bowen MA, Olsen KJ, Cheng L, Avila D, Podack ER. Functional effects of CD30 on a large granular lymphoma cell line. YT. Inhibition of cytotoxicity, regulation of CD28 and IL-2R, and induction of homotypic aggregation. *J Immunol* 1993;151:5896-906.
49. Hinz M, Lemke P, Anagnostopoulos I, Hacker C, Krappmann D, Mathas S, Dorken B, Zenke M, Stein H, Scheidereit C. Nuclear factor  $\kappa$ B-dependent gene expression profiling of Hodgkin's disease tumor cells, pathogenetic significance, and link to constitutive signal transducer and activator of transcription 5a activity. *J Exp Med* 2002;196:605-17.
50. Bargou RC, Leng C, Krappmann D, Emmerich F, Mapara MY, Bommer K, Royer HD, Scheidereit C, Dorken B. High-level nuclear NF- $\kappa$ B and Oct-2 is a common feature of cultured Hodgkin/Reed-Sternberg cells. *Blood* 1996;87:4340-7.
51. Cabannes E, Khan G, Aillet F, Jarrett RF, Hay RT. Mutations in the *I $\kappa$ B $\alpha$*  gene in Hodgkin's disease suggest a tumour suppressor role for I $\kappa$ B $\alpha$ . *Oncogene* 1999;18:3063-70.
52. Emmerich F, Meiser M, Hummel M, Demel G, Foss HD, Jundt F, Mathas S, Krappmann D, Scheidereit C, Stein H, Dorken B. Overexpression of I kappa B alpha without inhibition of NF- $\kappa$ B activity and mutations in the I kappa B alpha gene in Reed-Sternberg cells. *Blood* 1999;94:3129-34.
53. Krappmann D, Emmerich F, Kordes U, Scharschmidt E, Dorken B, Scheidereit C. Molecular mechanisms of constitutive NF- $\kappa$ B/Rel activation in Hodgkin/Reed-Sternberg cells. *Oncogene* 1999;18:943-53.
54. Gruss H-J, Pinto A, Gioghini A, Wehnes E, Wright B, Boiani N, Aldinucci D, Gattei V, Zagonel V, Smith CA, Kadin ME, von Schilling C, et al. CD30 ligand expression in nonmalignant and Hodgkin's disease-involved lymphoid tissues. *Am J Pathol* 1996;149:469-81.
55. Molin D, Fischer M, Xiang Z, Larsson U, Harvima I, Venge P, Nilsson K, Sundstrom C, Enblad G, Nilsson G. Mast cells express functional CD30 ligand and are the predominant CD30L-positive cells in Hodgkin's disease. *Br J Haematol* 2001;114:616-23.





ORIGINAL ARTICLE

## Nucleolin is involved in interferon regulatory factor-2-dependent transcriptional activation

A Masumi<sup>1</sup>, H Fukazawa<sup>2</sup>, T Shimazu<sup>3</sup>, M Yoshida<sup>3</sup>, K Ozato<sup>4</sup>, K Komuro<sup>1</sup> and K Yamaguchi<sup>1</sup>

<sup>1</sup>Department of Safety Research on Blood and Biological Products, National Institute of Infectious Diseases, Tokyo, Japan;

<sup>2</sup>Department of Bioactive Molecules, National Institute of Infectious Diseases, Tokyo, Japan; <sup>3</sup>Chemical Genetics Laboratory, RIKEN, Saitama, Japan and <sup>4</sup>Laboratory of Molecular Growth and Regulation, National Institute of Child Health and Human Development, National Institute of Health, Bethesda, MD, USA

We have previously shown that interferon regulatory factor-2 (IRF-2) is acetylated in a cell growth-dependent manner, which enables it to contribute to the transcription of cell growth-regulated promoters. To clarify the function of acetylation of IRF-2, we investigated the proteins that associate with acetylated IRF-2. In 293T cells, the transfection of p300/CBP-associated factor (PCAF) enhanced the acetylation of IRF-2. In cells transfected with both IRF-2 and PCAF, IRF-2 associated with endogenous nucleolin, while in contrast, minimal association was observed when IRF-2 was transfected with a PCAF histone acetyl transferase (HAT) deletion mutant. In a pull-down experiment using stable transfectants, acetylation-defective mutant IRF-2 (IRF-2K75R) recruited nucleolin to a much lesser extent than wild-type IRF-2, suggesting that nucleolin preferentially associates with acetylated IRF-2. Nucleolin in the presence of PCAF enhanced IRF-2-dependent *H4* promoter activity in NIH3T3 cells. Nucleolin knock-down using siRNA reduced the IRF-2/PCAF-mediated promoter activity. Chromatin immunoprecipitation analysis indicated that PCAF transfection increased nucleolin binding to IRF-2 bound to the *H4* promoter. We conclude that nucleolin is recruited to acetylated IRF-2, thereby contributing to gene regulation crucial for the control of cell growth.

*Oncogene* (2006) 25, 5113–5124. doi:10.1038/sj.onc.1209522; published online 3 April 2006

**Keywords:** IRF-2; nucleolin; acetylation

### Introduction

Interferon regulatory factors (IRFs) have been studied in the context of host defense and oncogenesis (Taniguchi *et al.*, 2001) and transcriptional regulation (Schaffer *et al.*, 1997). Interferon regulatory factor-2 (IRF-2) has generally been described as a transcriptional

repressor, and is thought to function by competing with the transcriptional activator IRF-1. However, IRF-2 can act as a positive regulator for interferon stimulated response element (ISRE)-like sequences such as the promoters *H4* (Vaughan *et al.*, 1998; Xie *et al.*, 2001), vascular adhesion molecule-1 and gp91phox (Luo and Skalnik, 1996) as well as Fas ligand (Chow *et al.*, 2000). Biologically, IRF-2 plays an important role in cell growth regulation, and has been shown to be a potential oncogene (Yamamoto *et al.*, 1994). A recent report indicated that IRF-2 drives megakaryocytic differentiation through regulation of the thrombopoietin receptor promoter (Stellacci *et al.*, 2004). It has been reported that many transcription factors, such as MyoD,  $\beta$ -catenin, p53, Tat and CTIIA regulate specific promoters associated with the coactivators p300 and p300/CBP-associated factor (PCAF), and that this regulation leads to specific biological functions (Lakin and Jackson, 1999; Deng *et al.*, 2000; Spilianakis *et al.*, 2000; Polwsskaya *et al.*, 2001; Wolf *et al.*, 2002). Certain IRF proteins interact with other transcription factors such as TFIIB, and the coactivators p300 and PCAF (Wang *et al.*, 1996; Yoneyama *et al.*, 1998; Masumi *et al.*, 1999) and these interactions lead to transcriptional activation or repression depending on the cell types involved. To clarify the regulatory functions of transcription factors, many investigators have studied the coactivators, such as p300 and PCAF.

There are many reports of the histone acetyltransferases such as PCAF, p300/CBP and GCN5 acting as co-activators (Benkirane *et al.*, 1998; Vassilev *et al.*, 1998; Hamamori *et al.*, 1999; Jiang *et al.*, 1999; Masumi *et al.*, 1999; Schiltz *et al.*, 1999; Harrod *et al.*, 2000; Lau *et al.*, 2000a,b; Li *et al.*, 2000; Trievel *et al.*, 2000; Yamauchi *et al.*, 2000; Vo and Goodman, 2001; Lang and Hearing, 2003; Patel *et al.*, 2004). A number of transcriptional factors associate with p300/CBP, originally known as the global co-activator, and with PCAF and GCN5. Recruitment of these histone acetylases is thought to alter chromatin structures, and is required as an integral part of transcriptional activation. As a result of interaction with histone acetylases, certain transcription factors become acetylated themselves, which often results in enhanced transcriptional activity (Sternier and Berger, 2000). We have previously reported that the

Correspondence: Dr A Masumi, Department of Safety Research on Blood and Biological Products, National Institute of Infectious Diseases, 4-7-1, Gakuen, Musashimurayama-shi, Tokyo 208-0011, Japan. E-mail: amasumi@nih.go.jp  
Received 30 June 2005; revised 22 February 2006; accepted 27 February 2006; published online 3 April 2006

transfection of PCAF-enhanced IRF-2-dependent *H4* promoter activity in NIH3T3 cells, (Masumi *et al.*, 1999) and that IRF-2 was acetylated by p300 and PCAF *in vivo* and *in vitro* (Masumi and Ozato, 2001), providing the first example of acetylation in the IRF family. Since then, additional IRF members IRF-3 and IRF-7, have been shown to be acetylated by p300 and PCAF, respectively, *in vivo* and *in vitro* (Caillaud *et al.*, 2002; Suhara *et al.*, 2002). Acetylation of IRF-2 leads to inhibition of histone acetylation by p300 *in vitro*, suggesting a possible mechanism for transcriptional repression by IRF-2 in U937 cells (Masumi and Ozato, 2001). In contrast, we demonstrated that acetylation of IRF-2 regulates cell growth by activation of the *H4* promoter (Masumi *et al.*, 2003). In NIH3T3 cells, IRF-2 associates with endogenous p300 and becomes acetylated, binds to an ISRE site, and activates *H4* promoter activity. Thus, we demonstrated that IRF-2 acts as repressor and activator through its acetylation. In this paper, which aimed to identify the protein that associates with acetylated IRF-2, we performed pull-down assay by using tagged a IRF-2 expression system and showed that IRF-2, acetylated by PCAF, recruits nucleolin and activates transcription. Nucleolin is reported to be a ubiquitously expressed multifunctional protein involved in ribosomal biogenesis and the regulation of nucleolar translocation of ribosomal proteins (Ginisty *et al.*, 1992; Srivastava and Pollard, 1999). Our results reveal a new function for nucleolin as an IRF-2-interacting partner and transcriptional activator.

**Results**

*Exogenous p300/CBP-associated factor acetylates interferon regulatory factor-2 in 293T cells*

We have demonstrated previously that IRF-2 acts as a transcriptional activator upon acetylation (Masumi *et al.*, 2003). To investigate IRF-2 acetylation by histone acetylases *in vivo*, flag-PCAF and flag-p300 were transfected into 293T cells with flag-IRF-2. Cells were labeled with <sup>14</sup>C-acetate 1 h before harvesting and a M2-agarose pull-down assay was performed (Figure 1). Western blot analysis of the immunoprecipitates using anti-flag M2 agarose indicated that these plasmid were expressed in 293T cells (Figure 1c). Western blot analysis of the immunoprecipitates using anti-flag M2 agarose showed that acetylation of flag-IRF-2 was enhanced by co-transfection with PCAF, and to a slightly lesser extent, by p300 (Figure 1a). The results from the incorporation of <sup>14</sup>C-acetate into p300, PCAF and IRF-2 in M2-agarose precipitates was in accordance with those seen with Western blotting (Figure 1b). The patterns of Western blotting with anti-acetyllysine antibody and the incorporation of <sup>14</sup>C-acetate in whole cell lysate transfected with any plasmid were almost similar between each lane (Figure 1a right and b right). To confirm that PCAF/histone acetyl transferase (HAT) acetylates IRF-2 in 293T cells, flag-PCAF and flag-PCAFΔHAT were transfected into 293T cells with flag-IRF-2. The pattern of Western blotting

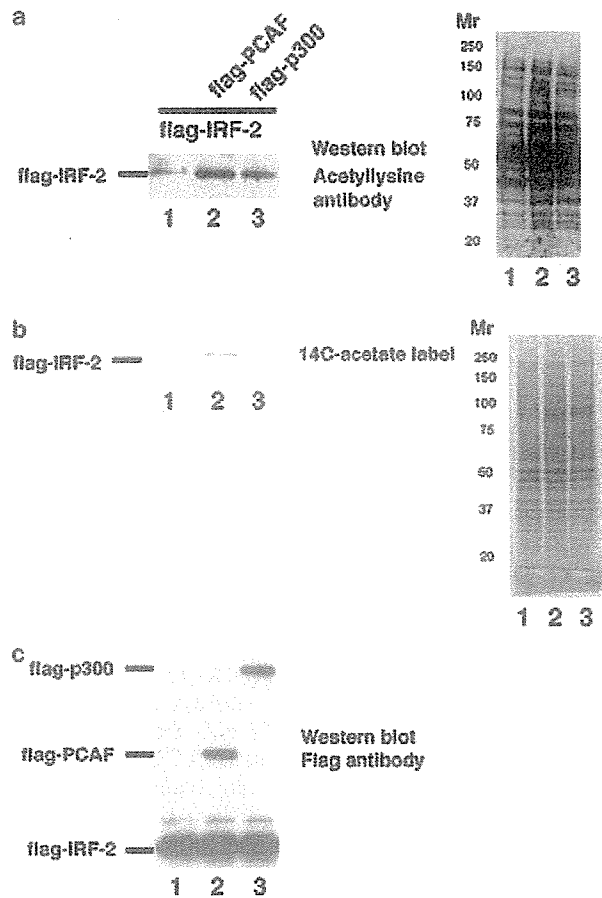


**Figure 1** Interferon regulatory factor-2 (IRF-2) is acetylated by p300/CBP-associated factor (PCAF) and p300 in 293T cells. (a) 293T cells were transfected with flag-IRF-2 (1 μg) (lanes 1–3), together with flag-PCAF (1 μg) (lane 2) and flag-p300 (1 μg) (lane 3) plasmids. Of <sup>14</sup>C-acetate, 20 μCi were added 1 h before preparation of the cell lysate. Cell lysates from 293T cells were incubated with M2-agarose, and then the flag-peptide elution fraction was electrophoresed on SDS-10% PAGE and immunoblotted using an anti-acetyl lysine antibody (left). Whole lysate was electrophoresed on SDS-10% PAGE and immunoblotted with anti-acetyl lysine antibody (right) (b) Immunoblotted membranes from M2-agarose precipitates (left) and whole lysate (right) were reused for Image analysis using a Fuji BAS 2500 to visualize the <sup>14</sup>C-incorporated protein. (c) Anti-flag M2 agarose precipitates from 293T transfected cells transfected with above plasmids were electrophoresed on SDS-10% PAGE and immunoblotted with an anti-flag antibody.

for whole cell lysates did not significantly affect the results (Figure 2b). Western blot analysis of the immunoprecipitates using anti-flag M2 agarose indicated that these protein were expressed in 293T cells (Figure 2a bottom). An M2-agarose pull-down assay showed that compared to the control vector, the acetylation level of IRF-2 was increased by transfection of full-length PCAF, but not by PCAF lacking HAT activity (Figure 2a top). We detected PCAF autoacetylation as described earlier (Santos-Rosa *et al.*, 2003). These results indicate that IRF-2 acetylation is enhanced by PCAFHAT *in vivo*.

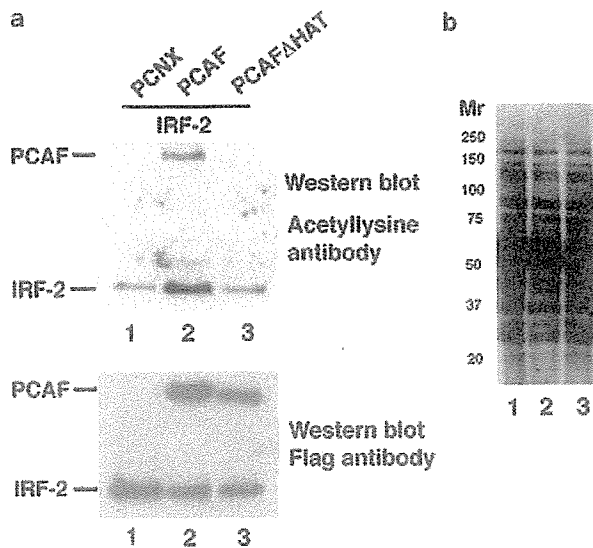


**Figure 2** Western blot analysis of 293T cells transfected with interferon regulatory factor-2 (IRF-2) and p300/CBP-associated factor (PCAF). (a) 293T cells were transfected with PCNX control vector (lane 1), flag-PCAF (lane 2) and flag-PCAFΔhistone acetyl transferase (HAT) (lane 3) with flag-IRF-2. An M2-agarose-purified fraction from cell lysate was separated on SDS-10% PAGE and immunoblotted with an anti-acetyllysine (upper panel) or anti-flag antibody (bottom panel). (b) Whole cell lysates from transfected 293T cells were electrophoresed and immunoblotted with an anti-acetyllysine antibody. Full-length PCAF was auto-acetylated as shown in lane 2.

*Interferon regulatory factor-2 recruits nucleolin in the presence of p300/CBP-associated factor*

Our previous report suggested that it is the involvement of cellular proteins associated with acetylated IRF-2, which results in its transcriptional regulation (Masumi *et al.*, 2003). To identify those proteins that associate with acetylated IRF-2, we performed an M2-agarose pull-down assay using 293T cells transfected with flag-IRF-2 and flag-PCAF. An M2-agarose-purified fraction was subjected to sodium dodecyl sulfate (SDS)-10% polyacrylamide gel electrophoresis (PAGE) and stained with Coomassie brilliant blue (Figure 3a). As shown in Figure 3a, proteins of approximately 110 and 70 kDa were observed in the immunoprecipitate from cells transfected with both flag-IRF-2 and flag-PCAF, but not in the immunoprecipitate from cells transfected with flag-PCAF alone. To identify these proteins, the bands were cut from the acrylamide gel, digested by trypsin and analysed by liquid chromatography-mass spectrometry/mass spectrometry (LC-MS/MS). Mass spectrometric analysis revealed that nucleolin was included in the 110-kDa band and that the heat shock protein 70 family was included in the 70 kDa band. As the heat shock protein 70 family is also included in the band in the PCAF-only transfected cells (Figure 3a, lane 1), we focused on nucleolin in this study. In Figure 3b, we investigated the nucleolin recruitment to IRF-2 using Western blotting. 293T cells were transfected with flag-IRF-2 in the presence or

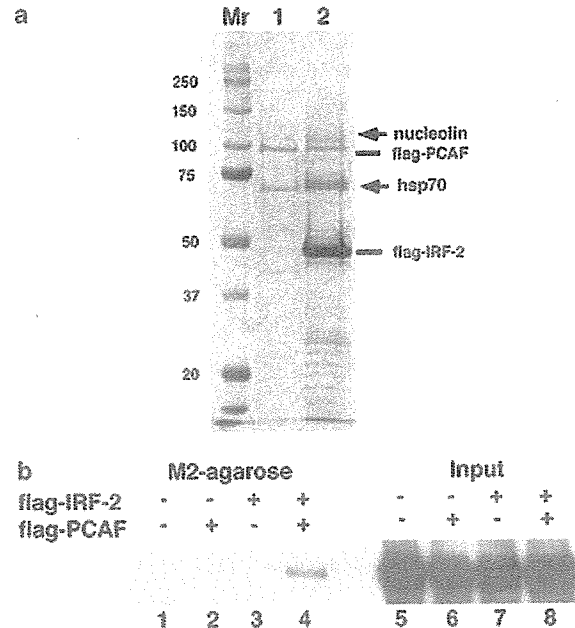


**Figure 3** Coomassie blue staining pattern of the proteins coprecipitated with flag-interferon regulatory factor-2 (IRF-2). (a) 293T cells were transfected with 5 μg flag-p300/CBP-associated factor (PCAF) (lane 1) alone and 5 μg flag-IRF-2 together with 5 μg flag-PCAF (lane 2). Whole cells were lysed in a buffer B and incubated with M2-agarose, and then the flag-peptide-eluted fraction was separated on SDS-10% PAGE and the gel was stained with Coomassie brilliant blue. The two bands indicated with arrows were cut and trypsinized, and then liquid chromatography-mass spectrometry/mass spectrometry (LC-MS/MS) analysis was performed. Nucleolin was included in the upper band and the hsp70 family was included in the lower band. (b) 293T cells were transfected with control vector (lane 1), flag-PCAF (lane 2), flag-IRF-2 (lane 3), and flag-IRF-2 and flag-PCAF (lane 4) as described in (a). Cell lysates from 293T cells were incubated with M2-agarose, and then the flag-peptide elution fraction was prepared. Whole cells (right) and M2-agarose precipitates (left) were immunoblotted with anti-nucleolin antibody.

absence of flag-PCAF, and then cell lysate was incubated with anti-flag M2-agarose. The flag-peptide-eluted fraction was immunoblotted with anti-nucleolin antibody. Nucleolin expression level was not altered in any plasmid-transfected 293T cells, and nucleolin was detected most clearly in the flag-peptide-eluted fraction from cells transfected with both flag-IRF-2 and flag-PCAF (Figure 3b).

We investigated whether the histone acetylase activity of PCAF was required to recruit nucleolin to IRF-2. Flag-IRF-2 was cotransfected with flag-PCAF or flag-PCAFΔHAT into 293T cells and precipitated with M2-agarose, then analysed for the amount of recruited nucleolin by Western blotting. There was no difference of the amount of nucleolin in the lysate of 293T cells transfected with any cDNA (Figure 4a). Nucleolin was clearly identified in the affinity-purified complex from IRF-2/PCAF-transfected cells, but not in the precipitates from IRF-2/PCAFΔHAT-, IRF-2 alone-, or PCAF alone-transfected cells (Figure 4a), consistent with the

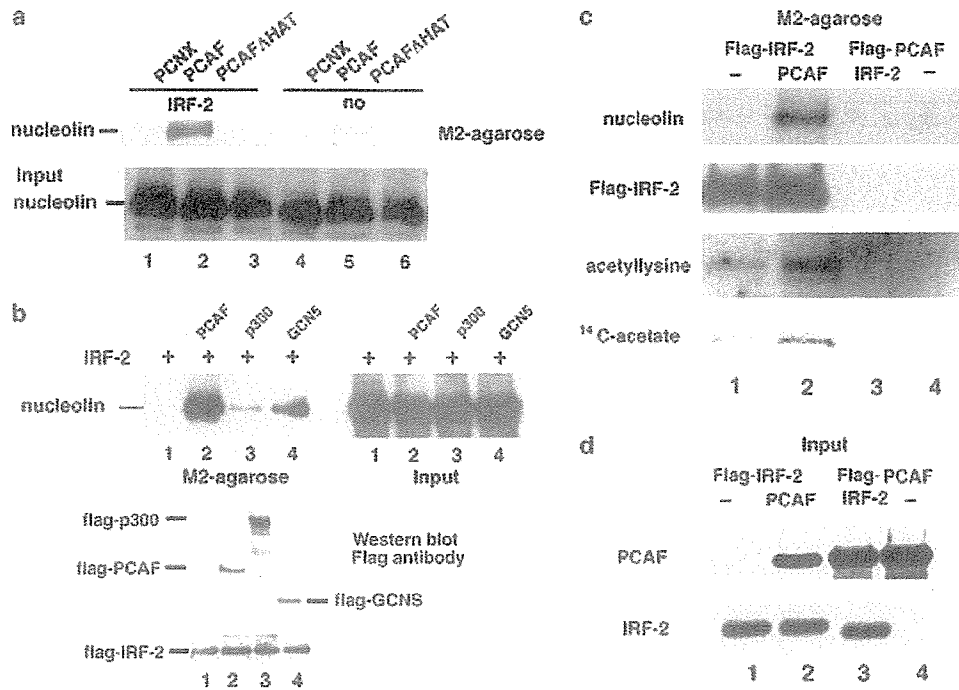


**Figure 4** Nucleolin is involved in an interferon regulatory factor-2 (IRF-2)-binding complex. (a) Cell lysates from 293T cells transfected with PCNX (lanes 1 and 4), flag-p300/CBP-associated factor (PCAF) (lanes 2 and 5) and flag-PCAF $\Delta$ histone acetyl transferase (HAT) (lanes 3 and 6), flag-IRF-2 (lanes 1–3) were incubated with M2-agarose and the flag-peptide-eluted fraction was separated on a SDS–10% PAGE and immunoblotted with anti-nucleolin antibody (upper panel). Whole cell lysates from transfected 293T cells were separated on SDS–10%PAGE and immunoblotted with an anti-nucleolin antibody (bottom panel). (b) 293T cells were transfected with PCNX empty vector (lane 1), flag-PCAF (lane 2), flag-p300 (lane 3) and flag-GCN5 (lane 4) in the presence of flag-IRF-2. Cell lysate was incubated with M2-agarose and the flag-peptide-eluted fraction was separated on a SDS–10% PAGE and immunoblotted with anti-nucleolin antibody (upper left panel). Whole cell lysates from transfected 293T cells were separated on SDS–10%PAGE and immunoblotted with an anti-nucleolin antibody (upper right panel). Anti-flag M2-agarose precipitates from transfected 293T cells were immunoblotted with anti-flag antibody (bottom panel). (c) Acetylated IRF-2 preferentially recruits nucleolin in 293T cells. Flag-IRF-2 was transfected into 293T cells in the absence or presence of PCAF (without tag) (lanes 1 and 2) or flag-PCAF was transfected with or without IRF-2 (without tag) (lanes 3 and 4).  $^{14}$ C-acetate was added to the 293T culture 1 h before harvesting. Cell lysates from 293T cells were incubated with M2-agarose and the flag-peptide fraction was electrophoresed and immunoblotted with anti-nucleolin, anti-flag, anti-acetyllysine antibodies. The membrane was reused for analysis with a BAS 2500 image analyzer to visualize  $^{14}$ C-labeled protein. (d) Western blot analysis of PCAF and IRF-2 for whole 293T cells transfected with flag-IRF-2 (lanes 1 and 2), flag-PCAF (lanes 3 and 4), IRF-2 (lane 3) and PCAF (lane 2) was performed.

results of Figure 3b. To test whether IRF-2 recruits nucleolin in the presence of other histone acetylases, the same amount of p300 and GCN5 was transfected into 293T cells with IRF-2. As shown in Figure 4b, transfection of flag-p300 and flag-GCN5 also induced nucleolin recruitment to flag-IRF-2, although p300 recruited nucleolin to a much lesser extent compared to other histone acetylases. For comparative nucleolin recruitment to IRF-2, greater amounts of p300 may be required because of its larger molecular size. Nucleolin is not detected in the flag-peptide-eluted fraction from cell lysate transfected with only flag-IRF-2 although IRF-2 is acetylated at basal level in the absence of exogenous PCAF in 293T cells (Figures 1–4). Detectable basal acetylation level of IRF-2 does not have enough binding affinity with nucleolin in 293T cells.

To further investigate these results, PCAF without a flag-tag was transfected with flag-IRF-2 into 293T cells and then an M2-agarose pull-down assay was performed. Nucleolin was recruited more potently to

affinity-purified precipitates of both flag-IRF-2 and PCAF-transfected cells than that of the cells transfected with flag-IRF-2 alone (Figure 4c). This result is similar to that was shown in Figure 4a. In addition, we detected an increase in IRF-2 acetylation in PCAF-transfected cells, consistent with the results in Figure 2. In contrast, when flag-PCAF was cotransfected with IRF-2 (without the flag-tag) into 293T cells, nucleolin was hardly detected in the anti-flag M2-agarose precipitates (Figure 4c).

We investigated whether an increased amount of PCAF transfection led to an increase in the recruitment of nucleolin to IRF-2. Differing amounts of PCAF was transfected into 293T cells with flag-tag IRF-2 and cell lysate was incubated with anti-flag M2 agarose, and the flag-peptide-eluted fraction was then immunoblotted with anti-acetyllysine, anti-nucleolin antibodies. Acetylation of IRF-2 and nucleolin recruitment increased parallel to amount of PCAF in 293T cells (Figure 5).